(12) INTERNATIONAL APPLICATION PUBLISHED UNDER THE PATENT COOPERATION TREATY (PCT)

(19) World Intellectual Property Organization
International Bureau

(43) International Publication Date
14 March 2013 (14.03.2013)

WIPO | PCT

(10) International Publication Number
WO 2013/034989 A2

(51) International Patent Classification:
A61K 48/00 (2006.01)

(21) International Application Number:
PCT/IB2012/002626

(22) International Filing Date:
7 September 2012 (07.09.2012)

(25) Filing Language: English

(26) Publication Language: English

(30) Priority Data:

61/531,942	7 September 2011 (07.09.2011)	US
61/696,981	5 September 2012 (05.09.2012)	US

(71) Applicants *(for all designated States except US)*: **3-D MATRIX, LTD.** [JP/JP]; Kojimachi-HF Bldg. 6F, Kojimachi 3-2-4, Chiyoda-ku, Tokyo, 102-0083 (JP). **NATIONAL CANCER CENTER RESEARCH INSTITUTE** [JP/JP]; 5-1-1, Tsukiji, Chuo-ku, Tokyo, 104-0045 (JP).

(72) Inventors; and

(75) Inventors/Applicants *(for US only)*: **OCHIYA, Takahiro** [JP/JP]; 5-1-1-218, Tsukiji, Chuo-ku, Tokyo, 104-0045 (JP). **FUJIWARA, Tomohiro** [JP/JP]; 6-3-2-305, Kachidoki, Chuo-ku, Tokyo, 104-0054 (JP).

(81) Designated States *(unless otherwise indicated, for every kind of national protection available)*: AE, AG, AL, AM, AO, AT, AU, AZ, BA, BB, BG, BH, BN, BR, BW, BY, BZ, CA, CH, CL, CN, CO, CR, CU, CZ, DE, DK, DM, DO, DZ, EC, EE, EG, ES, FI, GB, GD, GE, GH, GM, GT, HN, HR, HU, ID, IL, IN, IS, JP, KE, KG, KM, KN, KP, KR, KZ, LA, LC, LK, LR, LS, LT, LU, LY, MA, MD, ME, MG, MK, MN, MW, MX, MY, MZ, NA, NG, NI, NO, NZ, OM, PA, PE, PG, PH, PL, PT, QA, RO, RS, RU, RW, SC, SD, SE, SG, SK, SL, SM, ST, SV, SY, TH, TJ, TM, TN, TR, TT, TZ, UA, UG, US, UZ, VC, VN, ZA, ZM, ZW.

(84) Designated States *(unless otherwise indicated, for every kind of regional protection available)*: ARIPO (BW, GH, GM, KE, LR, LS, MW, MZ, NA, RW, SD, SL, SZ, TZ, UG, ZM, ZW), Eurasian (AM, AZ, BY, KG, KZ, RU, TJ, TM), European (AL, AT, BE, BG, CH, CY, CZ, DE, DK, EE, ES, FI, FR, GB, GR, HR, HU, IE, IS, IT, LT, LU, LV, MC, MK, MT, NL, NO, PL, PT, RO, RS, SE, SI, SK, SM, TR), OAPI (BF, BJ, CF, CG, CI, CM, GA, GN, GQ, GW, ML, MR, NE, SN, TD, TG).

Published:

— *without international search report and to be republished upon receipt of that report (Rule 48.2(g))*

— *with sequence listing part of description (Rule 5.2(a))*

(54) Title: MICRORNA-BASED METHODS AND ASSAYS FOR OSTEOSARCOMA

(57) Abstract: Provided are methods and compositions useful in the diagnosis, treatment, and monitoring of osteosarcoma. Antisense to certain microRNA (miRNA) found to be associated with cancer stem cells (CSCs) or tumor-initiating cells (TICs) of osteosarcoma are useful to suppress tumor growth and metastasis, and prolong survival. Antisense oligonucleotides to miR- 133a are synergistic in combination with standard chemotherapy such as cisplatin in the treatment of osteosarcoma.

MicroRNA-Based Methods and Assays for Osteosarcoma

RELATED APPLICATIONS

This application claims benefit of priority to United States Provisional Patent Application No. 61/531,942, filed September 7, 2011, and United States Provisional Patent Application No. 61/696,981, filed September 5, 2012.

BACKGROUND OF THE INVENTION

There is growing evidence that tumors contain a subset of cells with stem cell-like properties. These cells, often referred to either as "cancer stem cells" (CSCs) or as "tumor-initiating cells" (TICs), are responsible for forming the bulk of tumor. These CSCs possess both self-renewal and differentiation capabilities, and are believed to give rise to tumor heterogeneity. Furthermore, they have been shown to be associated with the most lethal characteristics of tumors — drug resistance and metastasis. The first evidence of the existence of CSCs came from studies of hematological malignancies in 1994. More recently, CSCs have been identified in a number of solid tumors, including breast, brain, skin, lung, colon, pancreatic, liver, head and neck, prostate, ovarian, and gastric cancers.

Osteosarcoma is the most common primary bone malignancy and accounts for 60% of all malignant childhood bone tumors. Before multi-agent chemotherapy, amputation provided a long-term survival rate of only ~20%. Since the 1970s, combination chemotherapy along with limb-sparing surgery has been the main treatment for osteosarcoma. Currently, the 5-year survival for patients with osteosarcoma has been reported to be 50% to 80%. However, this survival rate has not improved over the last 10 years, and fully 40% of osteosarcoma patients die of their disease.

Targeting molecules important in tumorigenesis, known as "targeted therapy", has been an exciting development in cancer treatment in the past ten years. However, no targeted therapy is currently available for osteosarcoma. Therefore, there is a great need for developing new osteosarcoma treatments.

CD133, also known as AC133 and Prominin 1 (PROM1), is a five-transmembrane glycoprotein of unknown function. It was the first identified member of the prominin family of five-transmembrane glycoproteins. In 1997, Yin et al. produced a novel monoclonal antibody that recognized the AC133 antigen, a glycosylation-dependent epitope of CD133, and they detected expression of AC133 in CD34-positive progenitor cells from adult blood. CD133 cDNA encodes a 5-transmembrane domain molecule with an extracellular N-terminus, a cytoplasmic C-terminus, and two large extracellular loops with eight consensus sites for N-linked glycosylation. A characteristic feature of CD133 is its rapid downregulation during cell differentiation. This feature makes CD133 a unique cell surface marker for the identification and isolation of stem cells and progenitor cells in several tissues. According to the CSC theory, CSCs express some of the stem cell markers of normal stem cells. Therefore, tumor cells expressing CD133 independently or in combination with other stem cell or progenitor cell markers are thought to represent CSCs. To date, however, the molecular mechanisms underlying the phenotype of CSCs expressing CD133 cell surface marker have remained obscure.

MicroRNAs (miRNAs), first discovered in 1993 as a small non-protein-coding RNA, are small regulatory RNA molecules that modulate the expression of their target genes and play important roles in a variety of physiological and pathological processes, such as development, differentiation, cell proliferation, apoptosis, and stress responses. miRNA biogenesis requires several post-transcriptional processing steps to yield the functional mature miRNA. Over the past several years, many miRNAs have been investigated in various human cancers. The deregulation of the expression of miRNAs has been shown to contribute to cancer development through various kinds of mechanisms, including deletions, amplifications, or mutations involving miRNA loci, epigenetic silencing, the dysregulation of transcription factors that target specific miRNAs, or the inhibition of processing. miRNA expression profiling is of increasing importance as a useful diagnostic and prognostic tool, and many studies have indicated that miRNAs act either as oncogenes or as tumor suppressors.

The human miRNAs miR-1 and miR-133a are located on the same chromosomal region, in a so-called cluster. Enriched in muscle, they are miRNAs that inhibit proliferation of progenitor cells and promote myogenesis by targeting histone deacetylase 4 (HDAC4) and serum response factor (SRF), respectively. miR-1 has been reported to be overexpressed in individuals with coronary artery disease, while both of these miRNAs have been reported to be expressed at low levels in cardiac hypertrophy. Despite a number of studies, their importance in muscle physiology and disease still remains unclear. Recently, miR-133a (the name of which bears no relationship to the name CD133) has been considered to be dispensable for the normal development and function of skeletal muscle. However, the relationship between these miRNAs and CSCs has, until now, been unknown.

The human miRNA miR-10b has been found to be positively associated with high-grade malignancy. This association held true for various types of cancer. miR-10b is one of the most significantly upregulated miRNAs in human pancreatic adenocarcinomas and glioblastomas, two types of highly metastatic and/or invasive cancers. This miRNA is highly expressed in metastatic cancer cells propagated as cell lines, as well as in metastatic breast tumors from patients, and is also upregulated in metastatic hepatocellular carcinomas relative to those that are not metastatic. The importance of miR-10b in sarcoma development has not previously been reported.

SUMMARY OF THE INVENTION

An aspect of the invention is a method of treating osteosarcoma. The method includes the step of administering to a subject in need thereof an effective amount of an antisense molecule specific for a microRNA (miRNA) selected from miR-1, miR-10b, and miR-133a.

In one embodiment, the antisense molecule is stabilized RNA.

In one embodiment, the stabilized RNA is a locked nucleic acid (LNA) oligonucleotide.

In one embodiment, the antisense molecule is DNA.

In one embodiment, the antisense molecule is 20-30 nucleotides long and comprises a nucleotide sequence at least 90 percent identical to 5′-ACATACTTCTTTACATTCCA-3′ (SEQ ID NO:4), 5′-ACAAATTCGGTTCTACAGGGT-3′ (SEQ ID NO:5), or 5′-CAGCTGGTTGAAGGGGACCAA-3′ (SEQ ID NO:6).

In one embodiment, the antisense molecule is 21-30 nucleotides long and comprises a nucleotide sequence at least 95 percent identical to 5′-ACATACTTCTTTACATTCCA-3′ (SEQ ID NO:4), 5′-ACAAATTCGGTTCTACAGGGT-3′ (SEQ ID NO:5), or 5′-CAGCTGGTTGAAGGGGACCAA-3′ (SEQ ID NO:6).

In one embodiment, the sequence of the antisense molecule is 5′-ACATACTTCTTTACATTCCA-3′ (SEQ ID NO:4),

5′-ACAAATTCGGTTCTACAGGGT-3′ (SEQ ID NO:5), or
5′-CAGCTGGTTGAAGGGGACCAA-3′ (SEQ ID NO:6).

In one embodiment, the antisense molecule is 20-30 nucleotides long and comprises a nucleotide sequence at least 90 percent identical to
5′-AUACAUACUUCUUUACAUUCCA-3′ (SEQ ID NO:7),
5′-CACAAAUUCGGUUCUACAGGGUA-3′ (SEQ ID NO:8),
5′-CAGCUGGUUGAAGGGGACCAAA-3′ (SEQ ID NO:9),
5′-ATACATACTTCTTTACATTCCA-3′ (SEQ ID NO:10),
5′-CACAAATTCGGTTCTACAGGGTA-3′ (SEQ ID NO:11), or
5′-CAGCTGGTTGAAGGGGACCAAA-3′ (SEQ ID NO:12).

In one embodiment, the antisense molecule is 21-30 nucleotides long and comprises a nucleotide sequence at least 95 percent identical to
5′-AUACAUACUUCUUUACAUUCCA-3′ (SEQ ID NO:7),
5′-CACAAAUUCGGUUCUACAGGGUA-3′ (SEQ ID NO:8),
5′-CAGCUGGUUGAAGGGGACCAAA-3′ (SEQ ID NO:9),
5′-ATACATACTTCTTTACATTCCA-3′ (SEQ ID NO:10),
5′-CACAAATTCGGTTCTACAGGGTA-3′ (SEQ ID NO:11), or
5′-CAGCTGGTTGAAGGGGACCAAA-3′ (SEQ ID NO:12).

In one embodiment, the sequence of the antisense molecule is
5′-AUACAUACUUCUUUACAUUCCA-3′ (SEQ ID NO:7),
5′-CACAAAUUCGGUUCUACAGGGUA-3′ (SEQ ID NO:8),
5′-CAGCUGGUUGAAGGGGACCAAA-3′ (SEQ ID NO:9),
5′-ATACATACTTCTTTACATTCCA-3′ (SEQ ID NO:10),
5′-CACAAATTCGGTTCTACAGGGTA-3′ (SEQ ID NO:11), or
5′-CAGCTGGTTGAAGGGGACCAAA-3′ (SEQ ID NO:12).

In one embodiment, the antisense molecule is associated with a nucleic acid delivery vehicle.

In one embodiment, the osteosarcoma is metastatic osteosarcoma.

An aspect of the invention is an isolated nucleic acid molecule 20-30 nucleotides long comprising a nucleotide sequence at least 90 percent identical to
5′-ACATACTTCTTTACATTCCA-3′ (SEQ ID NO:4),

5′-ACAAATTCGGTTCTACAGGGT-3′ (SEQ ID NO:5), or
5′-CAGCTGGTTGAAGGGGACCAA-3′ (SEQ ID NO:6).

In one embodiment, the isolated nucleic acid molecule is 21-30 nucleotides long and comprises a nucleotide sequence at least 95 percent identical to
5′-ACATACTTCTTTACATTCCA-3′ (SEQ ID NO:4),
5′-ACAAATTCGGTTCTACAGGGT-3′ (SEQ ID NO:5), or
5′-CAGCTGGTTGAAGGGGACCAA-3′ (SEQ ID NO:6).

In one embodiment, the sequence of the isolated nucleic acid molecule is
5′-ACATACTTCTTTACATTCCA-3′ (SEQ ID NO:4),
5′-ACAAATTCGGTTCTACAGGGT-3′ (SEQ ID NO:5), or
5′-CAGCTGGTTGAAGGGGACCAA-3′ (SEQ ID NO:6).

An aspect of the invention is an isolated nucleic acid molecule 20-30 nucleotides long comprising a nucleotide sequence at least 90 percent identical to
5′-AUACAUACUUCUUUACAUUCCA-3′ (SEQ ID NO:7),
5′-CACAAAUUCGGUUCUACAGGGUA-3′ (SEQ ID NO:8),
5′-CAGCUGGUUGAAGGGGACCAAA-3′ (SEQ ID NO:9),
5′-ATACATACTTCTTTACATTCCA-3′ (SEQ ID NO:10),
5′-CACAAATTCGGTTCTACAGGGTA-3′ (SEQ ID NO:11), or
5′-CAGCTGGTTGAAGGGGACCAAA-3′ (SEQ ID NO:12).

In one embodiment, the isolated nucleic acid molecule is 21-30 nucleotides long and comprises a nucleotide sequence at least 95 percent identical to
5′-AUACAUACUUCUUUACAUUCCA-3′ (SEQ ID NO:7),
5′-CACAAAUUCGGUUCUACAGGGUA-3′ (SEQ ID NO:8),
5′-CAGCUGGUUGAAGGGGACCAAA-3′ (SEQ ID NO:9),
5′-ATACATACTTCTTTACATTCCA-3′ (SEQ ID NO:10),
5′-CACAAATTCGGTTCTACAGGGTA-3′ (SEQ ID NO:11), or
5′-CAGCTGGTTGAAGGGGACCAAA-3′ (SEQ ID NO:12).

In one embodiment, the sequence of the isolated nucleic acid molecule is
5′-AUACAUACUUCUUUACAUUCCA-3′ (SEQ ID NO:7),
5′-CACAAAUUCGGUUCUACAGGGUA-3′ (SEQ ID NO:8),
5′-CAGCUGGUUGAAGGGGACCAAA-3′ (SEQ ID NO:9),

5′-ATACATACTTCTTTACATTCCA-3′ (SEQ ID NO:10),
5′-CACAAATTCGGTTCTACAGGGTA-3′ (SEQ ID NO:11), or
5′-CAGCTGGTTGAAGGGGACCAAA-3′ (SEQ ID NO:12).

In one embodiment, the nucleic acid molecule is associated with a nucleic acid delivery vehicle.

An aspect of the invention is a method of assessing resistance of osteosarcoma to an anti-cancer therapy. The method includes the steps of:

obtaining a tissue sample comprising osteosarcoma cells;

isolating from the sample cells expressing CD133;

measuring a first level of expression by the CD133-expressing cells of at least one microRNA (miRNA) selected from the group consisting of miR-1, miR-10b, and miR-133a;

contacting the CD133-expressing cells with an anti-cancer therapy; and

measuring a second level of expression by the CD133-expressing cells of the at least one miRNA, wherein a second level of expression greater than the first level of expression indicates the osteosarcoma is resistant to the anti-cancer therapy.

In one embodiment, the anti-cancer therapy is selected from the group consisting of cisplatin, doxorubicin, methotrexate, and any combination thereof.

An aspect of the invention is a method of screening for osteosarcoma. The method includes the step of performing on a tissue sample from a subject an assay specifically capable of detecting at least one microRNA (miRNA) selected from the group consisting of miR-1, miR-10b, and miR-133a, wherein detection by the assay of the presence in the sample of the at least one miRNA indicates the subject is at risk of having osteosarcoma.

In one embodiment, the tissue is blood.

In one embodiment, the tissue is serum.

An aspect of the invention is a method of monitoring osteosarcoma. The method includes the steps of:

(a) performing, on a tissue sample obtained from a subject having osteosarcoma or having been treated for osteosarcoma, an assay specifically capable of quantifying the level of expression of at least one microRNA (miRNA) selected from the group consisting of miR-1, miR-10b, and miR-133a; and

(b) repeating step (a) on a later-obtained tissue sample from the subject, wherein a level of expression of the at least one miRNA in the later-obtained sample greater than the level of expression of the at least one miRNA in the earlier-obtained sample indicates the osteosarcoma is progressive, and a level of expression of the at least one miRNA in the later-obtained sample lesser than the level of expression of the at least one miRNA in the earlier-obtained sample indicates the osteosarcoma is regressive.

In one embodiment, the tissue is blood.

In one embodiment, the tissue is serum.

BRIEF DESCRIPTION OF THE DRAWINGS

Figure 1 is a group of seven representative FACS analyses of various indicated human osteosarcoma cell lines based on their expression of CD133 (X-axis) and CD44 (Y-axis).

Figure 2 is a collage comprising a FACS analysis depicting selection of CD133^{high} and CD133^{low} SaOS2 cells (top panel); four photomicrographs depicting asymmetric cell division in the CD133^{high} population at day 1 and day 8 (middle panel); and two FACS analyses by PKH staining for each population at day 14 (bottom panel). Scale bars, 50 mm.

Figure 3 is a group of four photomicrographs and a bar graph depicting sphere-formation assays in freshly isolated CD133^{high} and CD133^{low} HOS-GFP cells. Photos were taken on day 5 and the numbers of spheres in each well were counted (n = 3 per group, $^{**}P < 0.01$). Scale bar, 200 μm.

Figure 4 is a bar graph depicting drug sensitivity of CD133^{high} and CD133^{low} SaOS2 cell populations. Relative viable cells to doxorubicin (DOX, 0.03 μM), cisplatin (CDDP, 2.5 μM), and methotrexate (MTX, 0.32 μM) were analyzed (n = 3 per group, $^{*}P < 0.05$, $^{**}P < 0.01$).

Figure 5 is a pair of photomicrographs and a bar graph depicting invasion assays in CD133^{high} and CD133^{low} SaOS2 cell populations (n = 3 per group, $^{**}P < 0.01$). Scale bar, 200 μm.

Figure 6 is a graph depicting quantitative polymerase chain reaction (qPCR) analysis of stem cell-associated, multiple drug-resistant transporters and metastasis-associated genes of CD133^{high} and CD133^{low} SaOS2 cell populations. β-actin was used as an internal control.

Figure 7 is a group of eight photographic images depicting tumorigenicity of CD133^{high} and CD133^{low} HOS-*luc* cell populations in mice. Luminescence of the tumors xenografted with CD133^{high} (animals' right thighs) and CD133^{low} (animals' left thighs) HOS-*luc* cells are identified by *in vivo* imaging system (IVIS). CD133^{high} population formed tumors with as few as 100 cells ($n = 5$ per group).

Figure 8 is a pair of FACS analyses depicting CD133^{high} cell populations in clinical osteosarcoma specimens.

Figure 9 is a graph depicting metastasis-free survival for osteosarcoma patients based on CD133 expression. Patients with high expression of CD133 had a median metastasis-free survival of less than 60 months ($n = 35$, log-rank test, $P = 0.0262$).

Figure 10 is a Venn diagram depicting upregulated and downregulated miRNAs in CD133^{high} and CD133^{low} cells of SaOS2 and HOS.

Figure 11 is a bar graph depicting upregulated miR-1, miR-10b, and miR-133a in CD133^{high} populations of SaO2 and HOS cells compared to CD133^{low} population ($^{*}P < 0.05$, $^{**}P < 0.01$, $^{***}P < 0.001$).

Figure 12 is a graph depicting the expression of miR-1, miR-10b, and miR-133a in CD133^{low} SaOS2 cells transfected with miRNA oligonucleotides compared to CD133^{low} SaOS2 cells transfected with miR-NC (negative control) oligonucleotides (log scale, $n = 3$ per group, $^{*}P < 0.05$, $^{**}P < 0.01$, $^{***}P < 0.001$).

Figure 13 is a graph depicting invasion assays in purified CD133^{low} cells transfected with miR-1, miR-10b, and miR-133a or NC oligonucleotides ($^{*}P < 0.05$, $^{**}P < 0.01$, $^{***}P < 0.001$).

Figure 14 is a graph depicting drug resistance in CD133^{low} cells transfected with miR-1, miR-10b, miR-133a, or miR-NC oligonucleotides (MTX, methotrexate at 0.22 mM; $^{*}P < 0.05$, $^{**}P < 0.01$).

Figure 15 is a schematic representation of plasmid vectors utilized for stable overexpression of miR-133a in CD133^{low} cells. NruI, NotI, XbaI: restriction endonuclease sites; P_{CMV}, cytomegalovirus promoter; MCS, multiple cloning site; IVS, intervening sequence; IRES, internal ribosome entry site; Hyg^{r}, hygromycin resistance gene; SV40 poly A, SV40 polyA tail.

Figure 16 comprises four pairs of photographic images depicting tumorigenicity of CD133^{low} HOS-*luc* cells stably expressing miR-133a (right legs) compared to control CD133^{low} HOS-*luc* cells (left legs). Each site was injected with the indicated number of cells (10^2-10^5); luminescent evaluation was performed 90 days post injection.

Figure 17 is a graph depicting expression of CD133 messenger RNA (mRNA) in CD133^{low} SaOS2 cells transfected with miR-1, miR-10b, and miR-133a oligonucleotides. Alteration of these miRNAs did not alter CD133 expression levels. Comparison is also made to CD133^{high} cells transfected with miR-NC (negative control) oligonucleotide ($n = 3$ per group).

Figure 18 is a graph depicting expression of miR-133a in CD133^{high} populations of freshly resected patient biopsies.

Figure 19 is a series of photomicrographs and a related bar graph depicting the effects of individual miRNAs, and various combinations of the miRNAs, on invasiveness of CD133^{low} SaOS2 cells transfected with the indicated miRNAs. For the purposes of comparison data is also presented for CD133^{high} SaOS2 cells. NC, negative control.

Figure 20 is a series of photomicrographs and related bar graph depicting the effects of individual miRNAs, and various combinations of the miRNAs, on invasiveness of CD133^{low} MNNG/HOS cells transfected with the indicated miRNAs. NC, negative control.

Figure 21 is a bar graph depicting proliferation of non-transfected CD133^{high} SaOS2 cells and CD133^{low} SaOS2 cells transfected with the indicated miRNAs. NC, negative control. Cells were maintained in culture for 4 d prior to counting.

Figure 22 comprises three graphs depicting (left) induction of mRNA for CD133 by doxorubicin (DOX) and cisplatin (CDDP) in 143B cells; (middle) induction of miR-1, miR-10b, and miR-133a by DOX in 143B cells; and (right) induction of miR-1, miR-10b, and miR-133a by CDDP in 143B cells ($*P < 0.05$, $**P < 0.01$, $***P < 0.001$).

Figure 23 is a pair of juxtaposed photographic images depicting tumorigenicity of cisplatin (CDDP)-treated CD133^{low} HOS-*luc* cells in mice. Luminescence of the tumors xenografted with CDDP-treated cells (animals' right tibias) and saline-treated control cells (animals' left tibias) are identified by *in vivo* imaging system (IVIS). CDDP-treated CD133^{low} cells formed tumors with as few as 100 cells ($n = 5$ per group).

Figure 24 is a graph depicting knock-down of miR-1, miR-10b, and miR-133 expression in CD133^{high} SaOS2 cells transfected with locked nucleic acid (LNA)-1, LNA-10b, LNA-133a, and LNA-NC oligonucleotides.

Figure 25 is a graph depicting cell proliferation on day 4 after transfection of LNA-133a and LNA-NC (negative control) oligonucleotides in CD133^{high} and CD133^{low} cells ($n = 3$ per group; $^{***}P < 0.001$).

Figure 26 is pair of graphs depicting (left) cell viability of indicated cell types grown in the presence of doxorubicin (DOX, 0.4 μM, 48 h) or cisplatin (CDDP, 5 μM, 48 h) measured 24 h after transfection with LNA-133a or LNA-NC; and (right) percentage of apoptotic cells in indicated cell types grown in the presence (+) or absence (-) of cisplatin (CDDP, 5 μM, 48 h) measured 24 h after transfection with LNA-133a or LNA-NC.

Figure 27 is a graph depicting invasion assays in indicated LNA-treated SaOS2 CD133^{high} and CD133^{low} populations ($n = 3$ per group; $^{**}P < 0.01$).

Figure 28 is a graph depicting quantitative polymerase chain reaction (qPCR) analysis of genes associated with stemness, drug resistance, and metastasis of osteosarcoma in CD133^{high} cells transfected with LNA-133a and LNA-NC oligonucleotides. β-actin was used as an internal control.

Figure 29 is a schematic depicting LNA-133a (LNA) and cisplatin (CDDP) administration schedule for 143B-*luc*-bearing mice. IVIS, *in vivo* imaging system.

Figure 30 is a graph depicting expression of miR-133a in 143B-*luc* tumors according to the dose of LNA-133a ($n = 3$ per group).

Figure 31 is a graph depicting relative expression of miR-133a in mice bearing 143B-*luc* tumors and treated with saline alone, LNA-133a alone, cisplatin (CDDP) alone, or LNA-133 plus CDDP ($^{*}P < 0.05$, $^{***}P < 0.001$).

Figure 32 is a group of four photographic images depicting macroscopic appearance, on day 36, of mice bearing 143B-*luc* tumors and treated with saline alone, LNA-133a alone, cisplatin (CDDP) alone, or LNA-133 plus CDDP. Scale bar, 10 mm.

Figure 33 is a graph depicting weight of 143B-*luc* tumors, on day 36, from each indicated treatment group ($^{**}P < 0.01$).

Figure 34 is a graph depicting survival of mice bearing 143B-*luc* tumors and treated with saline alone, LNA-133a alone, cisplatin (CDDP) alone, or LNA-133 plus CDDP. Kaplan-Meier analysis and log-rank test ($n = 5$ per group, $P = 0.0013$).

Figure 35 is a schematic depicting a strategy used to identify target genes of miR-133a. Anti-Ago2 IP, anti-Ago2 antibody immunoprecipitation.

Figure 36 is a Venn diagram depicting candidate target messenger RNAs (mRNAs) of miR-133a according to complementary DNA (cDNA) microarray and *in silico* database analysis.

Figure 37 is a graph depicting inhibition of cell growth by 10 siRNAs on cell transfection arrays in the presence of cisplatin 72 h after transfection ($n = 3$ per group; NC, negative control; $^{**}P < 0.01$, $^{***}P < 0.001$).

Figure 38 is a graph depicting invasion assay by 10 siRNAs on cell transfection arrays 72 h after transfection ($n = 3$ per group; NC, negative control; $^{*}P < 0.05$, $^{**}P < 0.01$, $^{***}P < 0.001$).

Figure 39 is a graph depicting luciferase activity in SaOS2 cells co-transfected with miR-133a oligonucleotides and luciferase reporters for the indicated putative miR-133a target genes.

Figure 40 is a graph depicting inverse correlation between expression of CD133 ($\mathrm{CD133}^{\mathrm{high}}$ versus $\mathrm{CD133}^{\mathrm{low}}$) and messenger RNA (mRNA) for indicated targets of miR-133a, as measured by quantitative reverse transcriptase-polymerase chain reaction (qRT-PCR).

Figure 41 is a graph depicting decreased expression of messenger RNA (mRNA) for the indicated miR-133a target genes in $\mathrm{CS133}^{\mathrm{low}}$ SaOS2 cells 48 h after transfection of miR-133a oligonucleotides compared to miR-NC (negative control) oligonucleotides, as measured by quantitative reverse transcriptase-polymerase chain reaction (qRT-PCR).

Figure 42 is a graph depicting increased expression of messenger RNA (mRNA) for SGMS2 in 143B-*luc* tumors from mice treated with LNA-133a (**$P < 0.01$).

Figure 43 is a series of six graphs depicting metastasis-free survival of osteosarcoma patients sensored for miR-133a target genes SGMS2, UBA2, SNX30, DUSP11, MAST4, and ANXA2, respectively. The low expression of the direct targets of miR-133a (except for DUSP11) were significantly correlated with a poor prognosis (Kaplan-Meier analysis and log-rank test; P values as shown).

DETAILED DESCRIPTION OF THE INVENTION

Since the proposal of the cancer stem cell (CSC) hypothesis, several studies have been performed to identify cancer stem cells of osteosarcoma. These cells have been detected in spherical clones under anchorage-independent, serum-starved culture conditions, as side population (SP) cells based on efflux of Hoechst 33342 dye or as CD117 and stro-1 cells sorted using cell surface marker. In view of these models, the inventors identified Prominin-1, the mouse homolog of human CD133, to be highly expressed in a small fraction of osteosarcoma cells. Cells from this CD133^{high} fraction formed cluster spheres in an anchorage-independent environment, exhibited a potential for self-renewal and differentiation, expressed stem cell-associated markers, and showed more invasive potential compared to the CD133^{low} fraction.

Following the characterization of the phenotype of osteosarcoma CSCs, the inventors profiled expression of several miRNAs, which distinguish cells of the CD133^{high} fraction from their more differentiated progeny. Among these miRNAs, miR-1, miR-10b, miR-133a were found to be upregulated in the CD133^{high} fraction compared to the CD133^{low} fraction of osteosarcoma cells. Remarkably, the inventors have discovered these miRNAs promote chemoresistance and invasiveness of osteosarcoma cells. These observations suggest that miR-1, miR-10b, and miR-133a are regulators of cancer stem cells of osteosarcoma. Particularly in combination with a tailored drug delivery system, new therapeutic agents (e.g., antisense nucleotides) targeting the miRNAs show great promise against osteosarcoma, adding to conventional chemotherapeutic agents, such as methotrexate, cisplatin, and doxorubicin.

Although miRNAs are not presently used as cancer therapeutics or as validated targets for cancer therapeutics, successful *in vivo* studies support the notion that they could be used as innovative therapeutics to address unmet needs. Systemic delivery of anti-miR-10b in an orthotopic mouse model of breast cancer showed a significant reduction in the number and size of lung metastases, with no obvious effect on primary tumors. Ma et al. (2010) *Nat Biotechnol* 28:341-7. Moreover, the recent discovery of miRNAs as novel biomarkers in serum or plasma represents a new approach for diagnostic screening in blood. Brase et al. (2010) *Mol Cancer* 9:306. The miRNAs identified in accordance with the instant invention also have potential as biomarkers which can be used for prompt assessment of sensitivity to chemotherapeutics, early detection of local recurrence, or distant metastasis, all of which are factors that affect the prognosis for patients with osteosarcoma.

An aspect of the invention is a method of treating osteosarcoma. The method includes the step of administering to a subject in need thereof an effective amount of an antisense molecule specific for a microRNA (miRNA) selected from miR-1, miR-10b, and miR-133a. Alternatively or in addition, the method can include the step of administering to the subject any agent that knocks down the expression of the miRNA.

As used herein, the terms "treating" and "to treat" refers to ameliorating or curing a disease or undesirable condition. For example, treating osteosarcoma refers to reducing or eliminating the burden of osteosarcoma cells in a subject having osteosarcoma.

A "subject" as used herein refers to a mammal. In one embodiment, a subject is a human.

An effective amount of an antisense molecule specific for a microRNA is administered to the subject in need of treatment. As used herein, an "effective amount" refers to an amount that is sufficient to achieve a desired biological outcome. For example, an effective amount to treat an osteosarcoma is an amount sufficient to reduce or eliminate the population of osteosarcoma cells in a subject having osteosarcoma. An effective amount may vary depending on such factors as the size of the tumor, the size of the subject, the overall condition of the subject, the route of administration, the identity of the active agent, the composition or formulation of the active agent, and other factors well known in the medical and pharmaceutical arts.

Without meaning to be bound to any particular dosage, an effective amount can, in general, vary from 0.01 microgram (μg)/kg body weight to 1000 mg/kg body weight of active agent per day when administered by a parenteral route of administration. For oral or enteral administration, an effective amount can, in general, vary from 0.1 μg/kg body weight to 10,000 mg/kg body weight of active agent per day. An effective amount can be determined, for example, based on *in vitro* studies and *in vivo* animal studies, as well as clinical studies.

MicroRNAs (miRNAs) are short (20-24 nt) non-coding RNAs that are involved in post-transcriptional regulation of gene expression in multicellular organisms by affecting both the stability and translation of mRNAs. miRNAs are transcribed by RNA polymerase II as part of capped and polyadenylated primary transcripts (pri-miRNAs) that can be either protein-coding or non-coding. The primary transcript is cleaved by the Drosha ribonuclease III enzyme to produce an approximately 70-nt stem-loop precursor miRNA (pre-miRNA), which is further cleaved by the cytoplasmic Dicer ribonuclease to generate the mature miRNA and antisense miRNA star (miRNA*) products. The mature miRNA is incorporated into an RNA-induced silencing complex (RISC), which recognizes target messenger RNAs (mRNAs) through imperfect base pairing with the miRNA and most commonly results in translational inhibition or destabilization of the target mRNA.

The miRNA can be selected from miR-1, miR-10b, and miR-133a. In one embodiment, the miRNA is miR-1. In one embodiment, the miRNA is miR-10b. In one embodiment, the miRNA is miR-133a. While these miRNAs have been described in the art, prior to the instant invention there was no recognition or expectation that these particular miRNAs are or might be associated with osteosarcoma, including, in particular, drug-resistant and/or aggressively invasive or metastatic phenotypes of osteosarcoma.

miR-1 has been described as a 22-nucleotide long miRNA having the sequence 5′-UGGAAUGUAAAGAAGUAUGUAU-3′ (SEQ ID NO:1).

miR-10b has been described as a 23-nucleotide long miRNA having the sequence 5′-UACCCUGUAGAACCGAAUUUGUG-3′ (SEQ ID NO:2).

miR-133a has been described as a 22-nucleotide long miRNA having the sequence 5′-UUUGGUCCCCUUCAACCAGCUG-3′ (SEQ ID NO:3).

Antisense is well described in the literature. In general, antisense agents are nucleic acid-based molecules having a nucleotide sequence that is complementary to the sequence of a target nucleic acid molecule, whereby association between the antisense molecule and its target sequence molecule results in a reduced amount of expression of the target nucleic acid molecule.

In one embodiment the antisense molecule (anti-miRNA) is a stabilized RNA, i.e., an RNA that, compared to naturally occurring RNA, is relatively resistant to nuclease-mediated degradation *in vitro* or *in vivo*. Numerous forms of stabilized nucleic acids, including RNA, are known. Some stabilized RNAs include polyA 3′-terminal ends. Chemically modified forms of nucleic acids, including, for example and without limitation, locked nucleic acids (LNAs), phosphorothioate backbone-modified nucleic acids, and 2′-*O*-methyl (2′-*O*Me) nucleic acids have been well described and require no further description here. Krützfeldt et al. (2005) *Nature* 438:685-9; Ma et al. (2010) *Nat Biotechnol* 28:341-7.

In one embodiment, the antisense molecule is a locked nucleic acid (LNA) oligonucleotide. A locked nucleic acid nucleotide is a modified ribonucleotide. The ribose moiety of an LNA nucleotide is modified with an extra bridge connecting the 2′ oxygen and 4′ carbon. The bridge "locks" the ribose in the 3′-*endo* conformation. LNA nucleotides were first developed by Imanishi and colleagues and Wengel and colleagues. Obika et al. (1997) *Tetrahedron Lett.* 38: 8735-8; Koshkin et al. (1998) *Tetrahedron* 54: 3607-30.

A locked nucleic acid (LNA) oligonucleotide is a polymer of nucleotides, at least one of which is an LNA nucleotide. Any non-LNA nucleotide in an LNA oligonucleotide can be a naturally occurring or modified ribonucleotide or deoxyribonucleotide, or an analog thereof, provided that the LNA oligonucleotide is functional as an antisense molecule with respect to its intended target. In one embodiment, any non-LNA nucleotide in an LNA oligonucleotide is a deoxyribonucleotide, and at least the 3′-terminal nucleotide is an LNA nucleotide. In one embodiment, any non-LNA nucleotide in an LNA oligonucleotide is a naturally occurring deoxyribonucleotide, and at least the two 3′-terminal nucleotides are LNA nucleotides. In one embodiment, an LNA oligonucleotide is composed exclusively of LNA nucleotides.

In one embodiment, the antisense molecule is DNA.

In one embodiment, an antisense molecule specific for miR-1 comprises a sequence 5′-ACATACTTCTTTACATTCCA-3′ (SEQ ID NO:4).

In one embodiment, the sequence of an antisense molecule specific for miR-1 is 5′-ACATACTTCTTTACATTCCA-3′ (SEQ ID NO:4).

In one embodiment, an antisense molecule specific for miR-10b comprises a sequence 5′-ACAAATTCGGTTCTACAGGGT-3′ (SEQ ID NO:5).

In one embodiment, the sequence of an antisense molecule specific for miR-10b is 5′-ACAAATTCGGTTCTACAGGGT-3′ (SEQ ID NO:5).

In one embodiment, an antisense molecule specific for miR-133a comprises a sequence 5′-CAGCTGGTTGAAGGGGACCAA-3′ (SEQ ID NO:6).

In one embodiment, the sequence of an antisense molecule specific for miR-133a is 5′-CAGCTGGTTGAAGGGGACCAA-3′ (SEQ ID NO:6).

In one embodiment, an antisense molecule specific for miR-1 comprises a sequence 5′-AUACAUACUUCUUUACAUUCCA-3′ (SEQ ID NO:7).

In one embodiment, the sequence of an antisense molecule specific for miR-1 is 5′-AUACAUACUUCUUUACAUUCCA-3′ (SEQ ID NO:7).

In one embodiment, an antisense molecule specific for miR-10b comprises a sequence 5′-CACAAAUUCGGUUCUACAGGGUA-3′ (SEQ ID NO:8).

In one embodiment, the sequence of an antisense molecule specific for miR-10b is 5′-CACAAAUUCGGUUCUACAGGGUA-3′ (SEQ ID NO:8).

In one embodiment, an antisense molecule specific for miR-133a comprises a sequence 5′-CAGCUGGUUGAAGGGGACCAAA-3′ (SEQ ID NO:9).

In one embodiment, the sequence of an antisense molecule specific for miR-133a is 5′-CAGCUGGUUGAAGGGGACCAAA-3′ (SEQ ID NO:9).

In one embodiment, an antisense molecule specific for miR-1 comprises a sequence 5′-ATACATACTTCTTTACATTCCA-3′ (SEQ ID NO:10).

In one embodiment, the sequence of an antisense molecule specific for miR-1 is 5′-ATACATACTTCTTTACATTCCA-3′ (SEQ ID NO:10).

In one embodiment, an antisense molecule specific for miR-10b comprises a sequence 5′-CACAAATTCGGTTCTACAGGGTA-3′ (SEQ ID NO:11).

In one embodiment, the sequence of an antisense molecule specific for miR-10b is 5′-CACAAATTCGGTTCTACAGGGTA-3′ (SEQ ID NO:11).

In one embodiment, an antisense molecule specific for miR-133a comprises a sequence 5′-CAGCTGGTTGAAGGGGACCAAA-3′ (SEQ ID NO:12).

In one embodiment, the sequence of an antisense molecule specific for miR-133a is 5′-CAGCTGGTTGAAGGGGACCAAA-3′ (SEQ ID NO:12).

The invention further embraces antisense molecules 20 to 30 nucleotides long comprising a contiguous sequence that is at least 90 percent identical to any one of the foregoing antisense molecule sequences. It is to be understood that such antisense molecules are capable of specifically hybridizing with or knocking down expression of the miRNAs to which they are targeted.

The invention further embraces antisense molecules 21 to 30 nucleotides long comprising a contiguous sequence that is at least 95 percent identical to any one of the foregoing antisense molecule sequences. It is to be understood that such antisense molecules are capable of specifically hybridizing with or knocking down expression of the miRNAs to which they are targeted.

In each of the foregoing embodiments, in one embodiment the antisense molecule includes one or more locked nucleic acid (LNA) nucleotides. Furthermore, in one embodiment the antisense molecule is composed exclusively of locked nucleic acid (LNA) nucleotides.

In one embodiment, the antisense molecule specific for a particular microRNA is associated with a nucleic acid delivery vehicle. As used herein, a "nucleic acid delivery vehicle" refers to a biologically compatible vector useful for delivering a nucleic acid molecule to the cytoplasm of a cell. The antisense molecule can be conjugated to the nucleic acid delivery vehicle. Alternatively or in addition, the antisense molecule can be encapsulated by the nucleic acid delivery vehicle. Examples of suitable nucleic acid delivery vehicles include liposomes, lipids, cholesterol, hormones, and other targeting molecules. In respect of liposomes, the antisense molecule can be associated with the outer surface of the liposome, the interior of the liposome, or both the exterior and the interior of the liposome.

In one embodiment, the osteosarcoma is localized osteosarcoma, e.g., osteosarcoma that is confined to one limb or one bone.

In one embodiment, the osteosarcoma is metastatic osteosarcoma.

An aspect of the invention is a method of assessing resistance of osteosarcoma to an anti-cancer therapy. The method includes the steps of

obtaining a tissue sample comprising osteosarcoma cells;

isolating from the sample cells expressing CD133;

measuring a first level of expression by the CD133-expressing cells of at least one microRNA (miRNA) selected from the group consisting of miR-1, miR-10b, and miR-133a;

contacting the CD133-expressing cells with an anti-cancer therapy; and

measuring a second level of expression by the CD133-expressing cells of the at least one miRNA, wherein a second level of expression greater than the first level of expression indicates the osteosarcoma is resistant to the anti-cancer therapy.

CD133-expressing cells can be isolated from a tissue sample using any suitable means. For example, a cell suspension can be prepared from the tissue and then the cells can be subjected to immunochromatography with, for example, magnetic beads loaded with anti-CD133 antibody, or by fluorescence-activated cell sorting (FACS) using an appropriately labeled anti-CD133 antibody. Monoclonal anti-human CD133 antibodies are commercially available from a number of suppliers.

A level of expression of a miRNA can be performed using any suitable method. For example, the expression level can be determined using reverse-transcriptase polymerase chain reaction (RT-PCR) using appropriately selected oligonucleotide primers. Alternatively or in addition, the expression level can be determined using Northern blotting with appropriately selected and labeled hybridization probe.

As used herein, an "anti-cancer therapy" refers to any modality of treatment useful to treat a cancer. Such modalities include, in general, chemotherapy, external beam radiation therapy, immunotherapy, hormone therapy, and combinations thereof. Chemotherapeutic agents are small molecules (molecular weight less than about 1 kDa) are well known in the medical arts. Commonly used chemotherapeutic agents used for osteosarcoma include cisplatin (*cis*-diamminedichloroplatinum (II), also known as CDDP, and cisplatinum, commercially available as Platinol and Platinol-AQ), doxorubicin (also known as hydroxydaunorubicin, commercially available as Adriamycin), and methotrexate (also known as amethopterin). In one embodiment, the anti-cancer therapy is selected from cisplatin, doxorubicin, methotrexate, and any combination thereof. Any two or more of these agents may be used in combination, either concurrently or sequentially. In addition, any one or combination of such anti-cancer therapies can be used in combination with another anti-cancer modality, for example, external beam radiation therapy.

In various embodiments, the osteosarcoma is identified as being resistant to the anti-cancer therapy when the second level of expression of at least one of miR-1, miR-10b, and miR-133a is objectively greater than the first level of expression. In various embodiments, the osteosarcoma is identified as being resistant to the anti-cancer therapy when the second level of expression of at least one of miR-1, miR-10b, and miR-133a is at least 10 percent, at least 20 percent, at least 30 percent, at least 40 percent, at least 50 percent, at least 60 percent, at least 70 percent, at least 80 percent, at least 90 percent, or at least 100 percent greater than the first level of expression.

In one embodiment, the method further comprises the step of adjusting the dose of or changing the anti-cancer therapy when the osteosarcoma is found to be resistant to the anti-cancer therapy. For example, when the osteosarcoma is found to be resistant to the anti-cancer therapy, the anti-cancer therapy can be supplemented with or changed to another suitable anti-cancer therapy.

An aspect of the invention is a method of screening for osteosarcoma. The method includes the step of performing on a tissue sample obtained from a subject an assay specifically capable of detecting at least one microRNA (miRNA) selected from the group consisting of miR-1, miR-10b, and miR-133a, wherein detection by the assay of the presence in the sample of the at least one miRNA indicates the subject is at risk of having osteosarcoma. In one embodiment, the miRNA is miR-1. In one embodiment, the miRNA is miR-10b. In one embodiment, the miRNA is miR-133a. In one embodiment, the at least one mi-RNA is any combination of miR-1, miR-10b, and miR-133a.

An assay specifically capable of detecting at least one microRNA (miRNA) selected from the group consisting of miR-1, miR-10b, and miR-133a can be, for example, RT-PCR using appropriately selected oligonucleotide primers. Alternatively or in addition, the assay can be Northern blotting with an appropriately selected and labeled hybridization probe.

In one embodiment, the tissue is blood. In one embodiment, the tissue is serum. In one embodiment, the tissue is plasma.

In one embodiment, the method further includes the step of verifying the presence of osteosarcoma, using any suitable method, when the subject is determined to be at risk of having osteosarcoma. For example, verifying the presence of osteosarcoma can include performing a skeletal survey or specific bone imaging analysis using X-rays or other suitable bone imaging technique, magnetic resonance imaging (MRI), computed tomography (CT), biopsy, and any combination thereof.

In one embodiment, the method further includes the step of treating the subject for osteosarcoma.

An aspect of the invention is a method of monitoring osteosarcoma. The method includes the steps of

(a) performing, on a tissue sample obtained from a subject having osteosarcoma or having been treated for osteosarcoma, an assay specifically capable of quantifying the level of expression of at least one microRNA (miRNA) selected from the group consisting of miR-1, miR-10b, and miR-133a; and

(b) repeating step (a) on a later-obtained tissue sample from the subject, wherein a level of expression of the at least one miRNA in the later-obtained sample greater than the level of expression of the at least one miRNA in the earlier-obtained sample indicates the osteosarcoma is progressive, and a level of expression of the at least one miRNA in the later-obtained sample lesser than the level of expression of the at least one miRNA in the earlier-obtained sample indicates the osteosarcoma is regressive.

An assay specifically capable of quantifying the level of expression of at least one microRNA (miRNA) selected from the group consisting of miR-1, miR-10b, and miR-133a can be, for example, RT-PCR using appropriately selected oligonucleotide primers.

In one embodiment, the tissue is blood. In one embodiment, the tissue is serum. In one embodiment, the tissue is plasma.

In one embodiment, the method further includes the step of adjusting the dose of or changing anti-cancer therapy when the osteosarcoma is found to be progressive. For example, when the osteosarcoma is found to be progressive, the anti-cancer therapy can be supplemented with or changed to another suitable anti-cancer therapy.

In one embodiment, the method further includes the step of adjusting the dose of or changing anti-cancer therapy when the osteosarcoma is found to be regressive. For example, when the osteosarcoma is found to be regressive, the anti-cancer therapy can be reduced or even suspended, or the anti-cancer therapy can be changed to another suitable anti-cancer therapy.

The invention, now having been generally disclosed, is further illustrated by the following non-limiting examples.

EXAMPLES

General Methods

Osteosarcoma cell purification from fresh clinical samples. Fresh human osteosarcoma samples were obtained in accordance with the ethical standards of the institutional committee on human experimentation from two patients undergoing diagnostic incisional biopsy from primary sites of osteosarcoma before neoadjuvant chemotherapy at the National Cancer Center Hospital of Japan between October 2010 and June 2011. The diagnosis of osteosarcoma and histologic subtypes were determined by certified pathologists. Surgical specimens were obtained at the time of resection and received in the laboratory within 10 minutes, immediately mechanically disaggregated and digested with collagenase and (Nitta-gelatin) and washed in phosphate-buffered saline (PBS) twice. Single-cell suspensions were obtained by filtration through a 70 µm filter (BD Biosciences). Cells were cultured in Dulbecco's modified Eagle's medium (DMEM) (Invitrogen) containing 10% heat-inactivated fetal bovine serum (FBS) (Gibco BRL) and penicillin (100 U/mL) and streptomycin (100 µg/mL) under 5% CO_2 in a in a humidified incubator at 37 °C.

Cells and cell culture. The human osteosarcoma HuO9 cell line was previously established in the applicant's laboratory. The human osteosarcoma cell lines SaOS2, U2OS, MG63, HOS, MNNG/HOS, and 143B were purchased from the American Type Culture Collection (ATCC). The transformed embryonic kidney cell line 293 was also obtained from the ATCC. SaOS2 and HuO9 cells were cultured in RPMI 1640 medium (Gibco BRL). U2OS, MG63, HOS, MNNG/HOS, 143B, and 293 cells were cultured in

DMEM (Invitrogen). All media were supplemented with 10% heat-inactivated FBS (Gibco BRL) and penicillin (100 U/mL) and streptomycin (100 μg/mL). The cells were maintained under 5% CO_2 in a humidified incubator at 37 °C.

Cell sorting and flow cytometry. Cell sorting by flow cytometry was performed on osteosarcoma cell lines and clinical samples using phycoerythrin (PE)-conjugated monoclonal mouse anti-human CD133/2 (293C3, Miltenyi Biotec) and allophycocyanin (APC)-conjugated monoclonal mouse anti-human CD44 (eBioscience). Isotype control mouse IgG1κ-PE (eBioscience) served as a control. Samples were analyzed and sorted on the JSAN cell sorter (Baybioscience) and the BD FACS AriaII (BD Biosciences). Viability was assessed using trypan blue exclusion. Results were analyzed with FlowJo software (Tree Star).

Cell proliferation and cytotoxity assay. Cell proliferation rates and cell viability as an indicator for the relative sensitivity of the cells to doxorubicin, cisplatin, and methotrexate were determined using TetraColor ONE Cell proliferation Assay System (Seikagaku) according to the manufacturer's instructions. Cells growing in the logarithmic phase were seeded in 96-well plates (5×10^3/well), allowed to attach overnight, and then were treated with varying doses of doxorubicin (Sigma), cisplatin (Alexis), and methotrexate (Sigma) for 72 h. Triplicate wells were used for each treatment group. Absorbance was measured at 450 nm with a reference wavelength at 650 nm on EnVision (Wallac). The relative number of viable cells was expressed as the percent of cell viability.

Sphere formation. Osteosarcoma cells were plated at 5,000-10,000 cells/well in 300 μL of serum-free DMEM/F12 medium (Invitrogen), supplemented with 20 ng/mL human recombinant epidermal growth factor (EGF) (Sigma-Aldrich), 10 ng/mL human recombinant basic fibroblast growth factor (bFGF) (Invitrogen), 4 μg/mL insulin (Sigma-Aldrich), B-27® (1:50; Invitrogen), 500 units/mL penicillin (Invitrogen), and 500 μg/mL streptomycin (Invitrogen). Cells were cultured in suspension in 24-well ultra-low attachment plates (Corning). Cells were replenished with 30 μL of supplemented medium every second day. Spheres were counted on day 5 in triplicate wells. Cell culture was carried out at 37 °C in a 5% CO_2 humidified incubator.

Invasion assay. Invasion assays were performed by using 24-well BD BioCoat Invasion Chambers with Matrigel (Becton-Dickinson). 1×10^5 cells, suspended in 500 μL

DMEM or RPMI 1640 medium without FBS, were added to the upper chamber, and DMEM or RPMI 1640 medium with 10% FBS was added to the lower chamber. After incubation for 24 h or 36 h, the cells on the upper surface of the filter were completely removed by wiping them with cotton swabs. The filters were fixed in methanol and stained with 1% toluidine blue in 1% sodium tetraborate (Sysmex). Filters were then mounted onto slides, and cells on lower surfaces were counted. Each assay was performed in triplicate.

miRNA profiling. miRNA expression profiling was performed using miRNA microarrays manufactured by Agilent Technologies (Santa Clara, CA), each containing 866 human miRNAs (Agilent Technologies [http://www.chem.agilent.com/scripts/PHome.asp]). Three independently extracted RNA samples of CD133^{high} and CD133^{low} cells just after isolation were used for array analyses in each cell line. Labeling and hybridization of total RNA samples were performed according to the manufacturer's protocol. Microarray results were extracted using Agilent Feature Extraction software (v10.7.3.1) and analyzed using GeneSpring GX 11.0.2 software (Agilent Technologies).

Clinical samples for survival correlation studies of CD133, miR-133a, and targets of miR-133a. Osteosarcoma tissue samples were obtained by diagnostic incisional biopsy from primary sites of osteosarcoma before neoadjuvant chemotherapy at the National Cancer Center Hospital of Japan between June 1997 and September 2010. Patients older than 40 y and having primary tumors located outside the extremities were excluded. Each fresh tumor sample was cut into two pieces, one of which was immediately cryopreserved in liquid nitrogen, and the other fixed with formalin. The diagnosis of osteosarcoma and histologic subtypes were determined by certified pathologists. Only osteosarcoma samples with the osteoblastic, chondroblastic, fibroblastic, and telangiectatic histologic subtypes were included. The response to chemotherapy was classified as good if the extent of tumor necrosis was 90% or greater. For the survival correlation studies of CD133 and the targets of miR-133a, available 35 cDNA samples from cDNA library were used, while RNA from available 48 formalin-fixed, paraffin-embedded (FFPE) samples were used for the correlation study of miR-133a. The clinical information of the patients is included in **Tables 7** and **10** (below). All patients provided written informed consent authorizing the collection and use of their samples for research purposes. The study protocol for obtaining clinical information and collecting samples was approved by the Institutional Review Board of the National Cancer Center of Japan.

RNA isolation and quantitative real-time RT-PCR of mRNAs and miRNAs. Total RNA was purified from cells and tumor tissues with an RNeasy Mini Kit and RNase-Free DNase Set (QIAGEN). For quantitative polymerase chain reaction (qPCR) of mRNAs, cDNA was synthesized using High-Capacity cDNA Reverse Transcription Kit (Applied Biosystems). For each qPCR reaction, equal amounts of cDNA were mixed with Platinum SYBER Green qPCR SuperMix (Invitrogen) and specific primers (**Table 1**). Gene expression levels were normalized by beta actin (ACTB) or glyceraldehyde 3-phosphate dehydrogenase (GAPDH). For qPCR of miRNAs, miRNA was converted to cDNA using the TaqMan MicroRNA Reverse Transcription Kit (Applied Biosystems). RNU6B small nuclear RNA was amplified as an internal control. qPCR was performed using each miRNA-specific probe included with the TaqMan MicroRNA Assay on a Real-Time PCR System 7300 and SDS software (Applied Biosystems).

Table 1. Sequences of primers for real-time RT-PCR analysis.

Gene	For/Rev	Sequence (5'-Sequence-3')	SEQ ID NO:
CD133	For	GGACCCATTGGCATTCTC	13
	Rev	CAGGACACAGCATAGAATAATC	14
Oct3/4	For	AGTGAGAGGCAACCTGGAGA	15
	Rev	ACACTCGGACCACATCCTTC	16
Nanog	For	CAGTCTGGACACTGGCTGAA	17
	Rev	CTCGCTGATTAGGCTCCAAC	18
Sox2	For	TGGTACGGTAGGAGCTTTGC	19
	Rev	TTTTTCGTCGCTTGGAGACT	20
ABCB1	For	CATGCTCCCAGGCTGTTTAT	21
	Rev	GTAACTTGGCAGTTTCAGTG	22
AGCG2	For	TGCAACATGTACTGGCGAAGA	23
	Rev	TCTTCCACAAGCCCCAGG	24
ABCC2	For	ACAGAGGCTGGTGGCAACC	25
	Rev	ACCATTACCTTGTCACTGTCCATGA	26
ezrin	For	CGGGACAAGTACAAGGCACTGCGGCAGATCCGG	27
	Rev	CCGGATCTGCCGCAGTGCCTTGTACTTCCG	28

β4-integrin	For	TGACGATCTGGACAACCTCAAGCA	29
	Rev	ATCCAATGGTGTAGTCGCTGGTGA	30
MMP13	For	GATACGTTCTTACAGAAGGC	31
	Rev	ACCCATCTGGCAAAATAAAC	32
CXCR4	For	GGAGGGGATCAGTATATACA	33
	Rev	GAAGATGATGGAGTAGATGG	34
SGMS2	For	CAATTCCTTGCTGCTTCTCC	35
	Rev	GCCTTTGTTTTGCTCCTCAG	36
UBA2	For	AAAAAGGGTGTGACCGAGTG	37
	Rev	GCATCTTCTTCCCCAAACAA	38
SNX30	For	CCTGAACGCCTACAAGAAGC	39
	Rev	ATGGTTCCCAGTTTGAGTGC	40
DOLPP1	For	GAGAGGAGTGAGGCAACAGG	41
	Rev	ACCCCAGACACAGGTTTGAG	42
DUSP11	For	GAGACGCGACTTTTCAGGAC	43
	Rev	GATCCAAAGGGGAAAAGCAT	44
CUL4B	For	GTTCTGGCGAAAAATCCAAA	45
	Rev	TCGAACAATTGCAGCATCA	46
ROD1	For	CATTCCTGGGGCTAGTGGTA	47
	Rev	CCATCTGAACCAAGGCATTT	48
ZNF701	For	ATCCCGTGGAGTGAAGGTC	49
	Rev	TCTCCAGCATCACGTCTCTG	50
MAST4	For	AGCCCATTTTTCATTTGCAC	51
	Rev	TCGTCTGGTGTTGGTTGGTA	52
ANXA2	For	CCTGAGCGTCCAGAAATGG	53
	Rev	GGACTGTTATTCGCAAGCTGGTT	54
ACTB	For	CATGAAGTGTGACGTGGACA	55
	Rev	CACGGAGTACTTGCGCTCAG	56
GAPDH	For	GACTTCAACAGCGACACCC	57
	Rev	GCCAAATTCGTTGTCATACCA	58

Transfection with synthetic miRNAs, LNAs, and siRNAs. Synthetic hsa-miRs (Pre-miR-hsa-miR-1, -10b, -133a, and negative control (NC; Applied Biosystems, **Table 2**) and locked nucleic acids (LNAs) (LNA-1, -10b, -133a, and negative control, Exiqon, **Table 3**) were transfected into each type of cells at 30 nM each (final concentration) using

DharmaFECT 1(GE Healthcare). Synthetic siRNAs (Bonac corporation, **Table 4**) were transfected into each type of cells at 100 nM each (final concentration) using DharmaFECT 1(GE Healthcare). After 24 hours of incubation, cells were treated with chemotherapeutic agents for cytotoxicity assay or reseeded into invasion chambers for invasion assay.

Table 2. Sequences of miRNA products

miRNA	Sense/Antisense	Sequence (5'-Sequence-3')	SEQ ID NO:
hsa-miR-1-2	Sense	UGGAAUGUAAAGAAGUAUUGUAU	1
	Antisense	UACAUACUUCUUAUGUACCC	59
hsa-miR-10b	Sense	UACCCUGUAGAACCGAAUUUGUG	2
	Antisense	ACAGAUUCGAUUCUAGGGGAAU	60
hsa-miR-133a-1	Sense	UUUGGUCCCCUUCAACCAGCUG	3
	Antisense	AGCUGGUAAAAUGGAACCAAAU	61

Table 3. Sequences of LNA products

miRNA	Sequence (5'-Sequence-3')	SEQ ID NO:
hsa-miR-1-2	ACATACTTCTTTACATTCCA	10
hsa-miR-10b	ACAAATTCGGTTCTACAGGGT	11
hsa-miR-133a-1	CAGCTGGTTGAAGGGGACCAA	12

Table 4. Sequences of siRNAs

Gene	Sense/Antisense	Sequence (5'-Sequence-3')	SEQ ID NO:
SGMS2	Sense	CCACUAGAGUGGUGGAAAAdTdT	62
	Antisense	UUUUCCACCACUCUAGUGGdTdT	63
UBA2	Sense	GGACUGGGCUGAAGUACAAdTdT	64
	Antisense	UUGUACUUCAGCCCAGUCCdTdT	65
SNX30	Sense	CCGAGAAGUUUGUGGUAAAdTdT	66
	Antisense	UUUACCACAAACUUCUCGGdTdT	67
DOLPP	Sense	CUUCCUAAUCCGAGACACAdTdT	68
	Antisense	UGUGUCUCGGAUUAGGAAGdTdT	69
DUSP11	Sense	CCAGAGGAUUUGCCAGAAAdTdT	70

	Antisense	UGUGUCUCGGAUUAGGAAGdTdT	71
CUL4B	Sense	GGUGAACACUUAACAGCAAdTdT	72
	Antisense	UUGCUGUUAAGUGUUCACCdTdT	73
ROD1	Sense	GGGAAUGACAGCAAGAAAUdTdT	74
	Antisense	AUUUCUUGCUGUCAUUCCCdTdT	75
ZNF701	Sense	CCAUAAUGAAGGAGGUCUUdTdT	76
	Antisense	AAGACCUCCUUCAUUAUGGdTdT	77
ANXA2	Sense	UGACCAAGAUGCUCGGGAUdTdT	78
	Antisense	AUCCCGAGCAUCUUGGUCAdTdT	79
MAST4	Sense	GGAGGUACCUUCUUCCAAAdTdT	80
	Antisense	UAUCAAACUUCCUCUUCUGdTdT	81

Establishment of miR-133a stably expressing cell line. miR-133a vectors were constructed by inserting cloning sequences including the full-length of the mature microRNA sequences into the pIRES-hyg vector (Clontech). The microRNA and control vectors were transfected into freshly isolated osteosarcoma $CD133^{low}$ HOS cells by calcium phosphate co-precipitation. The transfectants were split and grown in selective medium with 200 µg/mL of hygromycin. Hygromycin-resistant colonies were chosen and expanded in medium containing 200 µg/mL of hygromycin. The sequences of miR-133a constructs were confirmed by DNA sequencing (ABI 3130 sequencer, Applied Biosystems), and microRNA overexpression was confirmed by qRT-PCR. RNU6B served as the endogenous control.

Tumor transplantation experiments. Animal experiments were performed in compliance with the guidelines of the Institute for Laboratory Animal Research, National Cancer Center Research Institute. Athymic nude mice or NOD/SCID mice (CLEA Japan) were purchased at 4 weeks of age and given at least 1 week to adapt to their new environment prior to tumor transplantation. On day 0, mice were anesthetized with 3% isoflurane and the right leg disinfected with 70% ethanol. Cells were aspirated into a 1 mL tuberculin syringe fitted with a 27-G needle. The needle was inserted through the cortex of the anterior tuberosity of the tibia with a rotating movement to avoid cortical fracture. Once the bone was traversed, the needle was inserted further to fracture the posterior cortex of the tibia. A 100 µL volume of solution containing freshly isolated $CD133^{high}$ and

CD133^{low} HOS-Luc (10^2, 10^3, 10^4, 10^5 cells per site) or 143B-Luc (1.5×10^6) was injected while slowly moving back the needle.

Monitoring tumor growth, lung metastasis, and toxicity with/without LNA-anti-miR-133a. For the assessment of tumorigenicity between CD133^{high} and CD133^{low} HOS-Luc cells, NOD/SCID mice were injected with D-luciferin (150 mg/kg, Promega) by intraperitoneal injection. Ten minutes later, photons from firefly luciferase were counted using the IVIS imaging system (Xenogen Corp.) according to the manufacturer's instructions. Each experimental condition included 5 animals per group and monitoring once a week. For the evaluation of LNA-anti-miR-133a administration into spontaneous lung metastasis of osteosarcoma model mice, individual mice were injected with 10 mg/kg of LNA-anti-miR-133a or saline via the tail vain. LNA were injected on following days 4, 11, 18, 25, 32 postinoculation of 143B-Luc cells. Each experimental condition included 10 animals per group. The development of subsequent lung metastasis was monitored once a week *in vivo* by the bioluminescent imaging described above for 5 weeks. All data were analyzed using LivingImage software (version 2.50, Xenogen). On day 36, the primary tumor and lung in 5 mice of each group were resected at necropsy for their weight, bioluminescent, and histological analyses. The blood examination, weight of whole body as well as heart, liver, and skeletal muscle, and histopathological examination were performed for the assessment of toxicity. The remaining mice were observed for their survival period.

Comprehensive collection and identification of miR-133a target mRNAs. To collect comprehensive downstream targets of miR-133a, cDNA microarray profiling from two experimental approaches were performed. First, candidate genes were collected from cDNA microarray analysis performed from collected total RNA of SaOS2 CD133^{low} cells transduced with miR-133a or negative control (NC). Second, cDNA microarray analysis was performed from collected total RNA from anti-Ago2 antibody immunoprecipitation (Ago2-IP) in CD133^{low} cells transduced with miR-133a or NC. Downregulated genes in the former method with 1.5 fold decrease and upregulated genes in the latter method with 2.0 fold increase were defined as candidates by reference to *in silico* databases TargetScanHuman 6.0 (http://www.targetscan.org/).

Luciferase reporter assays. Each fragment of 3'UTR of SGMS2 (nt 1656-1879 (binding site) of NM_152621), UBA2 (nt 2527-2654 (binding site) of NM_005499), DUSP11 (nt 1180-1572 (binding site) of NM_003584), MAST4 (nt 8017-8096 (binding site) of NM_001164664), SNX30 (nt 6659-7611 (binding site) of NM_001012944) and CDS of ANXA2 (nt 244-743 (binding site) of NM_001002857) were amplified and cloned into the XhoI and NotI sites of firefly and renilla luciferase reporter genes of a psiCHECK-2 vector (Promega). All PCR products cloned into the plasmid were verified by DNA sequencing to ensure that they were free of mutations and in the correct cloning direction. Primer sequences are listed in **Table 5**. For the luciferase reporter assay, HOS cells were co-transfected with 100 ng of luciferase constructs and 100 nM synthetic miR-133a molecules or control (non-targeting siRNA oligonucleotide, Qiagen). Firefly and renilla luciferase activities were measured using the Dual-Luciferase Reporter Assay (Promega) 48 h after transfection. Results were expressed as relative renilla luciferase activity (renilla luciferase/firefly luciferase).

Table 5. Sequences of primers for luciferase reporter assays

Gene	For/Rev	Sequence (5'-Sequence-3')	SEQ ID NO:
SGMS2-UTR	For	GCTCGAGTAAAGCAAAACAAAGGCATCAGC	82
	Rev	GCGGCCGCAAGGCTTGTCACCAATGAATGA	83
SGMS2mu-UTR	For	AAATGTCAACCATTTTGTGTAAACGATTA	84
	Rev	AAATGGTTGACATTTCTTCATTTACCAG	85
UBA2-UTR	For	GCTCGAGTAATACCGCCTGGTATGTCTGTG	86
	Rev	GCGGCCGCAATGCAGATGCCATTTATTTGGT	87
UBA2mu-UTR	For	TTATGTCAACCATAAATGGCATCTGCATT	88
	Rev	TTATGGTTGACATAAGTATAGTCGTTAT	89
SNX30-1-UTR	For	GCTCGAGTAACCCTGTTGGACAGGATTGAT	90
	Rev	GCGGCCGCAATTTTTAAAGAAAGCATCTTTTATGG	91
SNX30mu-1-UTR	For	TCTTATCAACCCACTTCAGTCAGAAATGT	92
	Rev	AGTGGGTTGATAAGACTGCGAACAATCA	93
DUSP11-UTR	For	GCTCGAGTAAAAACCTGTCCTGGAATTCTACC	94
	Rev	GCGGCCGCAAGATGGCCTTTGGGTCAATAA	95
DUSP11mu-UTR	For	CTGGATCAACGAGCTGGCCTGAAAATTAC	96
	Rev	GCTCGTTGATCCAGGTAGAATTCCAGGA	97
MAST4-UTR	For	GCTCGAGTAACTCCCCCAGCTAGGAAACAG	98
	Rev	GCGGCCGCAAAGAGATGGGGCGGTCAGT	99

MAST4mu-UTR	For	GACGTTCAACCGCCATCCCCAGCCCCAAA	100
	Rev	TGGCGGTTGAACGTCTCTGCCCACGTTC	101
ANXA2-UTR	For	GCTCGAGTAAGCGGGATGCTTTGAACATT	102
	Rev	GCGGCCGCAACTCCAGCGTCATAGAGATCC	103
ANXA2mu-UTR	For	ATCAATCAACCAGGTGTGGATGAGGTCAC	104
	Rev	ACCTGGTTGATTGATGGCTGTTTCAATG	105

Immunohistochemistry. For the staining of CD133 and targets of miR-133a, slides of osteosarcoma clinical samples and xenografted tumors were prepared. Endogenous peroxidase was inhibited with 1% H_2O_2 (30 min). Slides were heated for antigen retrieval in 10 mM sodium citrate (pH 6.0). Subsequently, the slides were incubated with monoclonal mouse anti-human CD133/2 (1:10 dilution, Miltenyi Biotec), monoclonal mouse anti-human SGMS2 (1:50 dilution, Abcam), or isotype-matched control antibodies overnight at 4 °C. Immunodetection was performed using ImmPRESS peroxidase polymer detection reagents (Vector Laboratories) and Metal Enhanced DAB Substrate Kit (Thermo Fisher Scientific) according to the manufacturer's instructions. Staining was revealed by counter-staining with hematoxylin.

Statistical analysis. All statistical analyses were performed using SPSS software (SPSS, Inc.; Chicago, IL), with the exception of the significance in bar graphs, in which case analyses were performed by applying the Student's *t*-test. Differences in the CD133 expression among different clinicopathological data were analyzed by Chi-square (χ^2) test. Cases with ΔCt lower than the mean value were classified as having high CD133 expression, while cases with ΔCt higher than the mean value were classified as having low CD133 expression. The Kaplan-Meier method and the log-rank test were used to compare the survival of patients with CD133^{high} and CD133^{low} primary tumors. Survival period was defined as the time from diagnosis until death whereas living patients were censored at the time of their last follow-up. For the calculation of differences in the expressions of miR-133a and its targets, the same procedure was applied. In all these analyses, a *P* value of 0.05 or less was considered to be a significant difference.

Example 1

A Small Subset of Cells of Osteosarcoma Cell Line Expresses CD133

Osteosarcoma cell lines SaOS2, HOS, U2OS, MNNG/HOS, MG63, 143B, and HuO9 were screened for markers of mesenchymal stem cells or neural stem cells that have been considered as the origin of sarcoma. Basu-Roy, U et al. (2011) *Oncogene* 31:2270-82; Kuhn, NZ et al. (2010) *J. Cell. Physiol.* 222:268-77. As a result, CD133, the structural homolog of prominin-1, was found in all cell lines at a small population ranging from 0.04% to 8.47%, whereas CD44 was found in a large population (**Fig. 1**). SaOS2, MNNG/HOS, and HOS were found to be particularly strong in their expression of CD133 (8.47, 8.13, and 7.69 percent, respectively).

Single-cell proliferation of freshly isolated cell population was observed using PKH dye, which is a fluorescent dye that binds to cell membranes and segregates in daughter cells after each cell division. Normally, PKH concentration decreases with each cell division, so that quiescent cells remain PKH^{high} and dividing cells become progressively PKH^{low}. Moreover, normally PKH67 dye is distributed equally between daughter cells, whereas rapidly dividing cells, e.g., cancer cells, exhibit asymmetric division.

The $CD133^{high}$ cell population generated both $CD133^{high}$ and $CD133^{low}$ populations with different proliferative fates: one that is quiescent (PKH^{high}) and another that divides actively (PKH^{low}). A single $PKH26^{high}$ cell of $CD133^{high}$ fraction showed asymmetric division; a small number of $PKH26^{high}$ cells, presenting as dormant cells, were observed surrounded by $PKH26^{low}$ cells on day 8, which were identified as a fraction with both $CD133^{high}$ and $CD133^{low}$ cells on FACS analysis. On the other hand, a single $PKH67^{high}$ cell of $CD133^{low}$ SaOS2 fraction showed symmetric division; a colony with $PKH67^{low}$ cells was observed, which was identified as a $CD133^{low}$ fraction in FACS analysis two weeks after isolation (**Fig. 2**). No difference in cell division according to the expression of CD44 was observed.

Further examinations were performed to identify other phenotypes of $CD133^{high}$ and $CD133^{low}$ population. A total of 5×10^3 $CD133^{high}$ and $CD133^{low}$ cells were sorted and cultured immediately under conditions of serum-free, growth factor-supplemented anchorage-independent environment. Within two weeks of culture, more osteosarcoma spheres were observed from $CD133^{high}$ cells than $CD133^{low}$ cells (**Fig. 3**).

Example 2

CD133^{high} cells exhibit increased drug resistance, invasiveness, and tumorigenesis

Since drug resistance is one of the important properties of TICs, populations of CD133^{high} and CD133^{low} cells were observed in the treatment condition with doxorubicin (DOX), cisplatin (CDDP), and methotrexate (MTX), which are standard chemotherapeutics against osteosarcoma. CD133^{high} cells were more resistant to these chemotherapeutics than CD133^{low} cells (**Fig. 4**). Furthermore, CD133^{high} cells exhibited higher capability of invasion than CD133^{low} cells (**Fig. 5**). qRT-PCR of mRNA from freshly isolated CD133^{high} and CD133^{low} cells revealed that CD133^{high} SaOS2 cells expressed enhanced levels of *Oct3/4*, *Nanog*, and *Sox-2*, which are transcription factors that play a critical role in maintenance of self-renewal and pluripotency of embryonic stem cells as well as CSCs or TICs (Levings, PP et al. (2009) *Cancer Res.* 69:5648-55; Basu-Roy U et al. (2011) *Oncogene* 31:2270-82); multidrug resistance transporter genes *ABCB1*, *ABCC2*, *ABCG2*; and metastasis-associated genes *β4-integrin*, *ezrin*, *MMP-13*, and *CXCR4* (Tang, N et al. (2008) *Clin. Orthop. Relat. Res.* 466:2114-30; Osaki, M et al. (2011) *Mol. Ther.* 19:1123-30) (**Fig. 6**). Most importantly, the CD133^{high} HOS fraction showed stronger tumorigenicity *in vivo* than the CD133^{low} HOS fraction; CD133^{high} cells could form tumors from as few as 100 cells, whereas CD133^{low} cells could not (**Fig. 7**). Results are also shown in **Table 6.**

Table 6. Tumor development *in vivo* using osteosarcoma CD133^{high} and CD133^{low} populations alone

Cell Type	Tumor Incidence	Cell Number
CD133^{high}	5/5	100,000
	5/5	10,000
	5/5	1,000
	4/5	100
CD133^{low}	4/5	100,000
	1/5	10,000
	1/5	1,000
	1/5	100

Example 3

High-level expression of CD133 messenger RNA is a marker for poor survival rates of osteosarcoma patients

To evaluate the clinical importance of CD133, cell lines established from fresh human osteosarcoma biopsies were analyzed by flow cytometer and found to contain CD133^{high} population at a rare frequency <10% (**Fig. 8**). Furthermore, a clinical study of 35 osteosarcoma patients revealed that high expression levels of CD133 messenger RNA (mRNA) correlated with significantly worse overall survival rates of osteosarcoma patients (log-rank test, $P = 0.0262$). Results are shown in **Fig. 9** and **Table 7**.

Table 7. Uni- and multivariate analyses and the relationship between clinicopathologic variables and CD133 expression in 35 cases

Variable	Number of cases	CD133 Low	CD133 High	Correlation (CD133) χ^2 (*P* value)
Age (years)				0.120
0-10	7	6	1	
11-20	25	11	14	
21+	3	1	2	
Gender				0.164
Male	23	14	9	
Female	12	4	8	
Site				0.319
Femur	21	12	9	
Tibia	9	5	4	
Humerus	2	1	1	
Other	3	0	3	
Histology				0.394
Osteoblastic	16	9	7	
Chondroblastic	6	4	2	
Fibroblastic	2	0	2	
Other, NA*	11	5	6	
Metastasis at diagnosis				0.045
Present	4	0	4	
Absent	31	18	13	
Neoadjuvant chemotherapy				0.425
MTX+DOX/CDDP	21	10	11	

IFO+DOX/CDDP	13	8	5	
Other	1	0	1	
Response to neoadjuvant chemotherapy				0.088
Good (necrosis > 90%)	11	6	5	
Poor (necrosis < 90%)	20	12	8	
NA*	4	0	4	
CD133 mRNA expression				
High	17	0	17	
Low	18	18	0	

Example 4

miR-1, miR-10b, and miR-133a are upregulated in CD133^{high} cells compared to CD133^{low} cells

miRNA expression profiling has been reported to be a useful diagnostic and prognostic tool, and many studies have indicated that certain miRNAs act as either an oncogene or a tumor suppressor. Croce, CM (2009) *Nat. Rev. Genet.* 10:704-10. In order further to characterize the molecular mechanism underlying the CD133^{high} and CD133^{low} phenotypes, miRNA profiling of isolated CD133^{high} and CD133^{low} osteosarcoma SaOS2 and HOS cells was performed using microarray analysis containing 866 sequence-validated human miRNAs. Results, shown in **Fig. 10** and **Table 8**, revealed that 3 miRNAs were upregulated at >2-fold changes in CD133^{high} cells compared to CD133^{low} cells. A second round of qPCR validation study revealed miR-1, miR-10b, and miR-133a were consistent with the microarray data (**Fig. 11**).

Table 8. microRNA expression profile of CD133^{high} versus CD133^{low} osteosarcoma cells

miRNA	Fold change (SaOS2 CD133^{high} vs CD133^{low})	Regulation	Fold change (HOS CD133$_{high}$ vs CD133^{low})	Regulation
Commonly upregulated miRNAs in SaOS2 and HOS with >2 fold change in CD133^{high} cells compared to CD133^{low} cells				

hsa-miR-1	7.23	up	3.81	up
hsa-miR-500*	5.39	up	3.99	up
hsa-miR-660	2.09	up	2.05	up

Upregulated miRNAs in SaOS2 with >2 fold change in $CD133^{high}$ cells compared to $CD133^{low}$ cells

hsa-miR-551b	9.49	up
hsa-miR-30c	9.19	up
hsa-miR-148b	8.26	up
hsa-miR-193a-3p	7.77	up
hsa-miR-1	7.23	up
hsa-miR-221*	6.76	up
hsa-miR-24-1*	6.36	up
hsa-miR-1825	5.78	up
hsa-miR-500*	5.39	up
hsa-miR-92a-2*	4.36	up
hsa-miR-1202	3.39	up
hsa-miR-424	3.23	up
hsa-miR-19b-2*	2.87	up
hsa-miR-29c	2.42	up
hsa-miR-494	2.37	up
hsa-miR-10b	2.16	up
hsa-miR-374a	2.11	up
hsa-miR-660	2.09	up
hsa-miR-30e*	2.03	up

Downregulated miRNAs in SaOS2 with <2 fold change in $CD133^{high}$ cells compared to $CD133^{low}$ cells

hsa-miR-1281	9.45	down
hsa-miR-195	6.56	down
hsa-miR-129-5p	5.74	down
hsa-miR-129-3p	4.98	down
hsa-miR-183	4.89	down
hsa-miR-1305	4.76	down
hsa-miR-1275	4.65	down
hsa-miR-484	4.55	down
hsa-miR-1268	4.51	down
hsa-miR-186	4.51	down
hsa-miR-181a*	4.46	down
hsa-miR-744*	2.72	down
hsa-miR-96	2.65	down

hsa-miR-142-3p	2.35	down
hcmv-miR-US25-2-5p	2.31	down

Upregulated miRNAs in HOS with >2 fold change in $CD133^{high}$ cells compared to $CD133^{low}$ cells

hsa-miR-1181	12.78	up
hsa-miR-133b	7.22	up
hsa-miR-532-5p	7.10	up
hsa-miR-338-3p	6.30	up
hsa-miR-9	5.95	up
hsa-miR-34c-5p	5.37	up
hsa-miR-378*	5.26	up
hsa-miR-181a*	5.04	up
hsa-miR-145*	4.97	up
hsa-miR-1271	4.97	up
hsa-miR-362-3p	4.67	up
hsa-miR-152	4.63	up
hsa-miR-663	4.46	up
hsa-miR-9*	4.15	up
hsa-miR-340	4.10	up
hsa-miR-744	4.07	up
hsa-miR-500*	3.99	up
hsa-miR-1	3.81	up
hsa-miR-1305	3.33	up
hsa-miR-744*	3.11	up
hsa-miR-629	2.88	up
hsa-miR-629*	2.71	up
hsa-miR-145	2.55	up
hsa-miR-1246	2.47	up
hsa-miR-21*	2.39	up
hsa-miR-450a	2.35	up
hsa-miR-425*	2.31	up
hsa-miR-148a	2.30	up
hsa-let-7f-1*	2.26	up
hsa-miR-301b	2.21	up
hsa-miR-1826	2.15	up
hsa-miR-128	2.15	up
hsa-miR-378	2.14	up
hsa-miR-126	2.13	up
hsa-miR-598	2.06	up

hsa-miR-1915	2.05	up
hsa-miR-660	2.05	up
hsa-miR-933	2.02	up

Downregulated miRNAs in HOS with <2 fold change in CD133^{high} cells compared to CD133^{low} cells

hsv1-miR-H6	4.60	down
hsa-miR-1539	4.02	down
hsa-miR-483-3p	3.76	down
hsa-miR-328	3.72	down
hsa-miR-132*	3.67	down
hsa-miR-129*	3.66	down
hsa-miR-548c-5p	3.13	down
hsa-miR-1825	2.05	down

hsa, *Homo sapiens.*

miRNA and miRNA* are the two strands of the double-stranded RNA product of dicer processing of the stem loop precursor miRNA. miRNA is the "guide" strand that eventually enters RISC, and miRNA* is the other "passenger" strand. The level of miRNA* present in the cell is low ($\leq$ 15 % relative to the corresponding miRNA). In cases where there is a higher proportion of passenger strand present in the cell, the nomenclature miRNA-3p/miRNA-5p is used instead of miRNA/miRNA*. miRNA-3p is the miRNA derived from the 3' arm of the precursor miRNA, and miRNA-5p is the miRNA derived from the 5' arm of the precursor miRNA.

Example 5

Transfection of CD133^{low} cells with miR-133 confers properties associated with CD133^{high} cells, and high expression of miR-133a is correlated with poor clinical prognosis

To determine whether these miRNAs can inhibit these phenotypes of osteosarcoma tumor-initiating cells, expression levels of miR-1, miR-10b, and miR-133a were manipulated in CD133^{low} cells (**Fig. 12**). These miRNAs, especially miR-133a, enhanced the invasiveness of CD133^{low} cells compared to miR-NC (negative control) oligonucleotides (**Fig. 13**). Interestingly, transfection of all these miRNAs dramatically enhanced the invasion of CD133^{low} cells (**Fig. 13**). Cell proliferation and drug resistance were slightly enhanced in CD133^{low} cells by miR-133 transfection (**Fig. 14**). Stable overexpressing miR-133a HOS CD133^{low} cells (**Fig. 15**) showed stronger (> 2-fold) ability to form spheres than control CD133^{low} cells under anchorage serum-free environment and could develop tumors with as few as 100 cells *in vivo* whereas control CD133^{low} cells could not (**Fig. 16** and **Table 9**).

Table 9. Tumor development *in vivo* using osteosarcoma CD133^{low} populations stably overexpressing miR-133a

Cell Type	Tumor Incidence	Cell Number
CD133^{low} miR-133a	5/5	100,000
	4/4	10,000
	5/5	1,000
	2/5	100
CD133^{low} EV[1]	5/5	100,000
	1/4	10,000
	0/5	1,000
	0/5	100
CD133^{low} CDDP[2]	5/5	100
CD133^{low} Saline[3]	0/5	100

[1] EV, empty vector.

[2] CDDP, cells treated with CDDP.

[3] Saline, cells treated with saline.

Transfection of miR-133a also increased messenger RNA (mRNA) levels of the molecules that were upregulated in CD133^{high} cells (see **Fig. 6**) but not CD133 mRNA, suggesting that miR-133a does not affect the expression of the molecules on the upstream pathway of CD133 (**Fig. 17**). These results revealed that miR-133a is a candidate miRNA that can regulate the phenotypes of osteosarcoma TICs. Indeed, the expression of miR-133a was also high in the CD133^{high} fraction of osteosarcoma biopsies (**Fig. 18**), and high expression of miR-133a was significantly correlated with poor prognosis of patients (**Table 10**).

Table 10. Uni- and multivariate analyses and the relationship between clinicopathologic variables and miR-133a expression in 48 cases

Variable	Number of cases	miR-133a Low	miR-133a High	Correlation (CD133) χ^2 (P value)
Age (years)				0.228
0-10	9	9	0	
11-20	30	23	7	
21+	9	8	1	
Gender				1.000
Male	31	26	5	
Female	17	14	3	
Site				0.566
Femur	26	22	4	
Tibia	16	14	2	
Humerus	2	1	1	
Other	4	3	1	
Histology				0.142
Osteoblastic	25	23	2	
Chondroblastic	7	6	1	
Fibroblastic	2	2	0	
Other, NA*	14	9	5	
Metastasis at diagnosis				0.330
Present	7	5	2	
Absent	41	35	6	
Neoadjuvant chemotherapy				0.902
MTX+DOX/CDDP	29	24	5	
IFO+DOX/CDDP	18	15	3	
Other	1	1	0	
Response to neoadjuvant chemotherapy				0.173
Good (necrosis > 90%)	17	16	1	
Poor (necrosis < 90%)	26	21	5	
NA*	5	3	2	
miR-133a expression				
High	8	0	8	
Low	40	40	0	

Example 6

Transfection of CD133^{low} SaOS2 cells with miRNAs results in increased proliferation.

CD133^{low} SaOS2 cells were isolated by cell sorting and then transfected with negative control (NC) RNA, miR-1 alone, miR-10b alone, miR-133a alone, miR-1 plus mirR-10b, mirR-10b plus miR-133a, miR-1 plus miR-133a, or miR-1 plus miR-10b plus miR-133a. CD133^{high} cells also were isolated by cell sorting and then transfected with negative control (NC) RNA. Each population of cells was separately maintained in tissue culture for 3-7 days and then studied with a light microscope to assess cell proliferation. Results are shown in **Fig. 19**. As is evident from Fig. 19, CD133^{low} SaOS2 cells transfected with miR-1 alone, miR-10b alone, miR-133a alone, miR-1 plus mirR-10b, mirR-10b plus miR-133a, miR-1 plus miR-133a, or miR-1 plus miR-10b plus miR-133a proliferated to a greater extent than did CD133^{low} SaOS2 cells transfected with negative control RNA. CD133^{low} SaOS2 cells transfected with miR-1 plus miR-10b plus miR-133a proliferated to nearly the same extent as CD133^{high} cells transfected with negative control RNA. The effects of the combinations were at least additive.

Similar results were obtained in an experiment with MNNG/HOS cells in place of SaOS2 cells (**Fig. 20**).

Example 7

Transfection of CD133^{low} SaOS2 cells with miRNAs results in drug resistance

CD133^{low} SaOS2 cells were isolated by cell sorting and then transfected with negative control (NC) RNA, miR-1 alone, miR-10b alone, miR-133a alone, or miR-1 plus miR-10b plus miR-133a, similar to Example 1. Each population of transfected cells was then separately maintained in tissue culture for four days in the presence of 30 nM doxorubicin, 2.5 μM cisplatin, or 320 nM methotrexate, and then cells were counted. Results are shown in **Fig. 21**. As is evident from Fig. 21, CD133^{low} SaOS2 cells transfected with miR-133a alone or with miR-1 plus miR-10b plus miR-133a proliferated to a greater extent than negative control in the presence of cisplatin and in the presence of methotrexate. The addition of miR-133a thus was associated with increased resistance to cisplatin and methotrexate.

Example 8

miR-1, miR-10b, and miR-133a are induced by cisplatin treatment

The expressions of miR-1, miR-10b, and miR-133a, as well as CD133, were induced by cisplatin treatment. qRT-PCR analysis showed that DOX-treated or CDDP-treated (3 days) 143B cells expressed an increased level of miR-1, miR-10b, and miR-133a relative to untreated 143B cells (**Fig. 22**). In addition, the expression of miR-133a was enhanced by cisplatin in CD133^{low} HOS cells. Furthermore, exposure to CDDP increased *in vivo* tumorigenicity of CD133^{low} HOS population. CDDP-treated CD133^{low} HOS cells could form tumors with as few as 100 cells per injection, whereas the untreated CD133^{low} HOS cells could not (**Fig. 23** and **Table 9**). These data indicate that the TIC phenotypes, as well as the expression of CD133 mRNA and miR-133a, might be enhanced by chemotherapeutics. Therefore, we reasoned that silencing of miR-133a before or during chemotherapy would prevent the increase of the expression of miR-133a, which enhanced TIC phenotypes and was induced by chemotherapeutics.

Example 9

Antisense to miR-133a reduces proliferation of CD133^{high} cells

To evaluate whether silencing of miR-133a can suppress malignant phenotypes of osteosarcoma, experiments opposite those of Example 8 were performed by introducing locked nucleic acid (LNA) anti-miR-133a. LNA is a class of nucleic acid analogs possessing very high affinity and excellent specificity toward complementary DNA and RNA, and LNA oligonucleotides have been applied as antisense molecules both *in vitro* and *in vivo*. Elmèn, J et al. (2008) *Nature* 452:896-9; Obad, S et al. (2011) *Nat. Genet.* 43:371-8. CD133^{high} population of SaOS2 and HOS cells was isolated by cell sorting and transfected with LNA-anti-miR-133a (LNA-133a) and LNA-negative control (LNA-NC). As a control, the isolated CD133^{low} SaOS2 and HOS cells were also transfected with LNA-NC. The efficacy of LNA-133a for the silencing of miR-133a was confirmed by real-time RT-PCR analysis (**Fig. 24**). CD133^{high} SaOS2 and HOS cells transfected with LNA-133a were suppressed in proliferation rate to the same level of CD133^{low} cells transfected with LNA-NC (**Fig. 25**).

Example 10

LNA-133a-transduced CD133^{high} cells exhibit enhanced drug sensitivity and decreased invasiveness

LNA-133a-transduced CD133^{high} cells exhibited enhanced sensitivity to DOX and CDDP at the level of LNA-NC-transduced CD133^{low} cells. These results were validated by counting Hoechst-stained cells showing apoptotic nuclear condensation and fragmentation in CD133^{high} cells. There was a significantly higher apoptotic cell death rate in LNA-133a-transduced CD133^{high} cells compared to control CD133^{high} cells (**Fig. 26**). Furthermore, LNA-133a decreased the invasiveness of CD133^{high} SaOS2 and HOS populations (**Fig. 27**) and the expression of the molecules associated with CD133^{high} phenotypes (**Fig. 28**). Collectively, these observations suggest that silencing of miR-133a in CD133^{high} cells can reduce the malignant phenotype of osteosarcoma TICs, including drug resistance and invasion.

Example 11

Silencing of miR-133a in vivo is effective for the treatment of osteosarcoma and exhibits synergistic efficacy in combination with CDDP

To extend the *in vitro* findings and to determine whether silencing of miR-133a could be an effective therapeutic option for osteosarcoma treatment, the effect of LNA-133a on a spontaneous lung metastasis model of osteosarcoma was examined. Experimentally, 1.5 x 10^6 cells of 143B transfected with firefly luciferase gene (143B-*luc*) were implanted orthotopically into the right proximal tibia of athymic nude mice. The implanted tumor growth and the presence of distant metastases were analyzed weekly for luciferase bioluminescence using an *in vivo* imaging system (IVIS). A new treatment protocol was made of LNA-133a intravenous (i.v.) administration (10 mg kg^{-1}) 24 h before intraperitoneal (i.p.) injection of CDDP (2.5 mg kg^{-1}) (**Fig. 29**) in order to decrease drug resistance and to prevent the induction of TIC phenotypes by chemotherapy, which were observed in *in vitro* experiments. Before the animal study of this protocol, we confirmed reduced miR-133a levels in osteosarcoma tissues from LNA-133a-treated mice compared with those from saline-treated mice (**Fig. 30**). To assess the efficacy of the new treatment protocol, results were compared with three control groups ($n = 10$ each): a saline control group, an LNA group, and a CDDP group. At 5 weeks, half the mice in each group were euthanized for further analysis; the remaining mice were monitored for survival.

Results. The expression of miR-133a of tumors was decreased in the presence of LNA-133a (**Fig. 31**). Mice that had been administered LNA-133a (10 mg kg^{-1} i.v.) and CDDP (2 mg kg^{-1} i.p.) showed a significantly smaller tumor growth compared to the other groups (**Figs. 32** and **33**). No significant differences in tumor growth were observed in the presence or in the absence of CDDP alone (**Figs. 32** and **33**). Furthermore, lung metastasis was observed in 10/10 (100%) of the saline group, 7/10 (70%) of the LNA group, 8/10 (80%) of CDDP group, and only 3/10 (30%) of combination group (LNA-133a + CDDP) on day 35 (**Table 11**).

Table 11. Outcome of LNA treatment in osteosarcoma-bearing mice

Group	Tumor weight (mean) (g)	Lung metastasis	Luminescence of lung (mean)
ctrl.	3.928	10 / 10	5047
LNA	3.143	7 / 10	1744
CDDP	3.957	8 / 10	2855
LNA + CDDP	1.901	3 / 10	582

The average luminescence at chest region was significantly decreased in mice treated with the combination of LNA-133a and CDDP. Both the number and size of lung metastasis at every lobe were validated in the luciferase assay and histopathological examination.

Notably, the effect of the combination therapy (LNA-133a + CDDP) was found to exhibit synergistic inhibition of lung metastasis.

Furthermore, the combination therapy (LNA-133a + CDDP) significantly extended the survival period of tumor-bearing mice (log-rank test, $P = 0.0084$, **Fig. 34**). Despite the highly conserved sequence of mature human miR-133a and murine miR-133a (e.g., GenBank Accession No. NR_029676; 5′-UUUGGUCCCCUUCAACCAGCUG-3′; SEQ ID NO:3), all mice showed minimal toxic effects on various tissue including heart, liver, and skeletal muscle during the observation period. Thus, systemic administration of LNA-133a is effective for suppression of tumor growth and lung metastasis in the xenograft model for highly metastatic osteosarcoma in the presence of cisplatin.

Example 12

Identification of gene targets for miR-133a

The examples above establish that miR-133a regulates the malignancy of CD133^{high} osteosarcoma TICs, and inhibition of miR-133a expression in osteosarcoma cells inhibits the tumor development. In order to understand the mechanisms regulated by miR-133a in CD133^{high} osteosarcoma TICs, candidate mRNA expression profiling was performed by two different microarray analyses together with *in silico* predictions (**Fig. 35**). We detected 1812 downregulated genes with at least a 1.2-fold decrease in the first microarray analysis of total RNA collected from SaOS2 CD133^{low} cells transduced miR-133a or NC, whereas 4976 upregulated genes were detected with at least a 2.0-fold increase in the second microarray analysis of mRNA expression in RNA collected from anti-Ago2 antibody immunoprecipitation in CD133^{low} cells transduced with miR-133a or NC (**Fig. 36**). Subsequently, 226 genes were collected by both methods (**Table 12**), and 20 genes were identified in TargetScanHuman 6.0, one of the publicly available *in silico* databases (**Fig. 36**).

Table 12. Predicted gene targets for miR-133a by two analyses of cDNA microarray and *in silico* prediction

Gene Symbol	GenBank Accession	Gene Name	Fold increase, miR-133a-Ago2 complex	Fold decrease, miR-133a transfection
PGAP1	NM_024989	post-GPI attachment to proteins 1	7.60	-0.42
C1orf118	XR_041258	chromosome 1 open reading frame 118	7.19	-0.28
DYNLT3	NM_006520	dynein, light chain, Tctex-type 3	7.17	-0.42
AGFG1	NM_001135187	ArfGAP with FG repeats 1	6.69	-0.28
WDR44	NM_019045	WD repeat domain 44	6.36	-0.43
FLYWCH1	NM_020912	FLYWCH-type zinc finger 1	5.62	-0.32
CARKD	NM_018210	carbohydrate kinase domain containing	5.50	-0.66
CUL4B	NM_003588	cullin 4B	5.30	-0.40
ETS1	NM_005238	v-ets erythroblastosis virus E26 oncogene homolog 1 (avian)	5.29	-0.74

HDAC6	NM_006044	histone deacetylase 6	5.20	-0.36
C19orf10	NM_019107	chromosome 19 open reading frame 10	5.17	-0.36
RASA2	NM_006506	RAS p21 protein activator 2	5.15	-0.44
KIAA1958	NM_133465	KIAA1958	5.14	-0.28
LOC645851	NR_024395	hypothetical LOC645851	5.09	-0.37
TBPL1	NM_004865	TBP-like 1	4.86	-0.33
SNX26	NM_052948	sorting nexin 26	4.73	-0.27
SCRN1	NM_001145513	secernin 1	4.72	-0.55
LOC100132672	XR_038504	similar to glycosyltransferase 8 domain containing 3	4.61	-0.36
AP4S1	NM_001128126	adaptor-related protein complex 4, sigma 1 subunit	4.39	-0.59
SF3B3	NM_012426	splicing factor 3b, subunit 3, 130kDa	4.34	-0.27
LMBR1	NM_022458	limb region 1 homolog (mouse)	4.31	-0.40
HERC4	NM_022079	hect domain and RLD 4	4.26	-0.69
ADAMTS1	NM_006988	ADAM metallopeptidase with thrombospondin type 1 motif, 1	4.17	-0.47
CYB5R4	NM_016230	cytochrome b5 reductase 4	4.14	-0.29
LHFPL2	NM_005779	lipoma HMGIC fusion partner-like 2	4.11	-0.30
FAM13AOS	NR_002806	FAM13A opposite strand (non-protein coding)	4.04	-0.28
RALGAPA1	NM_194301	Ral GTPase activating protein, alpha subunit 1 (catalytic)	4.00	-0.53
TNFRSF13C	NM_052945	tumor necrosis factor receptor superfamily, member 13C	3.99	-0.44
LOC100131829	AK124002	hypothetical protein LOC100131829	3.95	-0.43
C1orf58	NM_144695	chromosome 1 open reading frame 58	3.92	-0.54
TNFRSF10D	NM_003840	tumor necrosis factor receptor superfamily, member 10d, decoy with truncated death domain	3.75	-0.45
ZDHHC17	NM_015336	zinc finger, DHHC-type containing 17	3.68	-0.36
LOC729603	NR_003288	calcium binding protein P22 pseudogene	3.62	-0.34
SNX30	NM_001012994	sorting nexin family member 30	3.55	-0.41
TSTD2	NM_139246	thiosulfate sulfurtransferase (rhodanese)-like domain containing 2	3.52	-0.38
SPRYD4	NM_207344	SPRY domain containing 4	3.51	-0.35
PTPMT1	NM_175732	protein tyrosine phosphatase, mitochondrial 1	3.50	-0.38
KLHDC4	NM_017566	kelch domain containing 4	3.43	-0.43
SLC30A7	NM_133496	solute carrier family 30 (zinc transporter), member 7	3.38	-0.48
TCEA3	NM_003196	transcription elongation factor A (SII), 3	3.32	-0.39
GORASP1	NM_031899	golgi reassembly stacking protein 1, 65kDa	3.17	-0.51

RBM15B	NM_013286	RNA binding motif protein 15B	3.13	-0.80
PDGFRB	NM_002609	platelet-derived growth factor receptor, beta polypeptide	3.13	-0.37
ITPRIPL2	NM_001034841	inositol 1,4,5-triphosphate receptor interacting protein-like 2	3.09	-0.34
FBXO3	NM_033406	F-box protein 3	3.01	-0.35
FAM122B	NM_001166600	family with sequence similarity 122B	3.00	-0.30
MINPP1	NM_004897	multiple inositol polyphosphate histidine phosphatase, 1	2.98	-0.28
SPOPL	NM_001001664	speckle-type POZ protein-like	2.94	-0.47
FAM86B1	NM_001083537	family with sequence similarity 86, member B1	2.85	-0.44
LOC100128071	XM_001724939	similar to hCG41624	2.83	-0.31
CCNT1	NM_001240	cyclin T1	2.82	-0.53
AP2M1	NM_004068	adaptor-related protein complex 2, mu 1 subunit	2.80	-0.44
AKIRIN1	NM_024595	akirin 1	2.73	-0.27
CHMP5	NM_016410	chromatin modifying protein 5	2.69	-0.61
PPM1K	NM_152542	protein phosphatase 1K (PP2C domain containing)	2.67	-0.53
MICALL2	NM_182924	MICAL-like 2	2.66	-0.29
DGKZ	AK123378	diacylglycerol kinase, zeta 104kDa	2.65	-0.39
SCARNA16	NR_003013	small Cajal body-specific RNA 16	2.65	-0.50
SERPINE1	NM_000602	serpin peptidase inhibitor, clade E (nexin, plasminogen activator inhibitor type 1), member 1	2.65	-0.61
STARD13	NM_178006	StAR-related lipid transfer (START) domain containing 13	2.58	-0.28
ROD1	NM_005156	ROD1 regulator of differentiation 1 (S. pombe)	2.55	-0.36
VEGFC	NM_005429	vascular endothelial growth factor C	2.45	-0.35
MYH9	NM_002473	myosin, heavy chain 9, non-muscle	2.43	-0.39
CCNJ	NM_019084	cyclin J	2.41	-0.26
WDR66	NM_144668	WD repeat domain 66	2.38	-0.32
CSRNP1	NM_033027	cysteine-serine-rich nuclear protein 1	2.34	-0.28
MYBL1	NM_001144755	v-myb myeloblastosis viral oncogene homolog (avian)-like 1	2.32	-0.29
EME2	BC041011	essential meiotic endonuclease 1 homolog 2 (S. pombe)	2.31	-0.44
MGC27382	AK091757	hypothetical MGC27382	2.27	-0.33
MMP14	NM_004995	matrix metallopeptidase 14 (membrane-inserted)	2.27	-0.42
WASH1	NM_182905	WAS protein family homolog 1	2.26	-0.32
RIMS2	NM_014677	regulating synaptic membrane exocytosis 2	2.25	-0.45
HSPG2	NM_005529	heparan sulfate proteoglycan 2	2.25	-0.45

HDAC8	NM_018486	histone deacetylase 8	2.21	-0.34
AK2	NM_013411	adenylate kinase 2	2.20	-0.30
SRRM2	NM_016333	serine/arginine repetitive matrix 2	2.19	-0.28
LOC731419	XM_001132610	hypothetical protein LOC731419	2.19	-0.32
SYNGR3	NM_004209	synaptogyrin 3	2.11	-0.33
PRUNE2	NM_015225	prune homolog 2 (Drosophila)	2.11	-0.38
MLKL	NM_152649	mixed lineage kinase domain-like	2.10	-0.30
DST	NM_001723	dystonin	2.10	-0.44
PBXIP1	NM_020524	pre-B-cell leukemia homeobox interacting protein 1	2.03	-0.78
ANTXR2	NM_058172	anthrax toxin receptor 2	1.98	-0.61
NSF	NM_006178	N-ethylmaleimide-sensitive factor	1.98	-0.32
APH1A	NM_001077628	anterior pharynx defective 1 homolog A (C. elegans)	1.98	-0.34
RASA1	NM_002890	RAS p21 protein activator (GTPase activating protein) 1	1.95	-0.46
BAIAP2	NM_017451	BAI1-associated protein 2	1.91	-0.29
GARNL3	NM_032293	GTPase activating Rap/RanGAP domain-like 3	1.90	-0.49
CKLF	NM_016951	chemokine-like factor	1.89	-0.38
SNORD17	NR_003045	small nucleolar RNA, C/D box 17	1.88	-0.27
TRIT1	NM_017646	tRNA isopentenyltransferase 1	1.88	-0.43
FILIP1L	NM_182909	filamin A interacting protein 1-like	1.88	-0.36
VAMP2	NM_014232	vesicle-associated membrane protein 2 (synaptobrevin 2)	1.87	-0.31
TBL1X	NM_005647	transducin (beta)-like 1X-linked	1.87	-0.30
LOC729314	XR_037423	similar to POM121-like protein 1	1.85	-0.63
RHD	NM_016124	Rh blood group, D antigen	1.84	-0.28
HERC2	NM_004667	hect domain and RLD 2	1.81	-0.36
KIAA1967	NM_021174	KIAA1967	1.78	-0.32
YIPF2	NM_024029	Yip1 domain family, member 2	1.71	-0.48
MLL5	NM_182931	myeloid/lymphoid or mixed-lineage leukemia 5 (trithorax homolog, Drosophila)	1.71	-0.41
DUSP11	NM_003584	dual specificity phosphatase 11 (RNA/RNP complex 1-interacting)	1.70	-0.28
ABL2	NM_001100108	v-abl Abelson murine leukemia viral oncogene homolog 2 (arg, Abelson-related gene)	1.68	-0.30
RBMX2	NM_016024	RNA binding motif protein, X-linked 2	1.65	-0.37
ALS2CR8	NM_024744	amyotrophic lateral sclerosis 2 (juvenile) chromosome region, candidate 8	1.65	-0.30
IDH1	NM_005896	isocitrate dehydrogenase 1 (NADP+), soluble	1.65	-0.31

NT5C3L	NM_052935	5'-nucleotidase, cytosolic III-like	1.63	-0.40
ERMP1	NM_024896	endoplasmic reticulum metallopeptidase 1	1.59	-0.86
GPSM1	NM_015597	G-protein signaling modulator 1 (AGS3-like, C. elegans)	1.53	-0.47
ARHGEF10L	NM_018125	Rho guanine nucleotide exchange factor (GEF) 10-like	1.52	-0.32
MFN2	NM_014874	mitofusin 2	1.52	-0.32
CG030	NR_026928	hypothetical CG030	1.49	-0.30
UBXN7	NM_015562	UBX domain protein 7	1.49	-0.35
CCDC45	NM_138363	coiled-coil domain containing 45	1.47	-0.39
ZNF701	NM_018260	zinc finger protein 701	1.46	-0.68
LOC642406	AK024257	similar to contactin associated protein-like 3B	1.46	-1.34
PHF8	NM_015107	PHD finger protein 8	1.44	-0.28
MED23	NM_015979	mediator complex subunit 23	1.42	-0.29
ARHGAP11B	NM_001039841	Rho GTPase activating protein 11B	1.42	-0.29
MYST4	NM_012330	MYST histone acetyltransferase (monocytic leukemia) 4	1.41	-0.31
SYT17	NM_016524	synaptotagmin XVII	1.40	-0.39
DPM2	NM_003863	dolichyl-phosphate mannosyltransferase polypeptide 2, regulatory subunit	1.30	-0.35
TUB	NM_003320	tubby homolog (mouse)	1.30	-0.27
TBPL1	NM_004865	TBP-like 1	1.30	-0.28
FAM40B	NM_020704	family with sequence similarity 40, member B	1.30	-0.62
DOLPP1	NM_020438	dolichyl pyrophosphate phosphatase 1	1.29	-0.34
HIST1H2BM	NM_003521	histone cluster 1, H2bm	1.29	-0.35
ZBTB7A	NM_015898	zinc finger and BTB domain containing 7A	1.28	-0.28
SLC30A7	NM_133496	solute carrier family 30 (zinc transporter), member 7	1.25	-0.36
HCRTR1	NM_001525	hypocretin (orexin) receptor 1	1.22	-0.27
DNAJB6	NM_005494	DnaJ (Hsp40) homolog, subfamily B, member 6	1.22	-0.56
QPRT	NM_014298	quinolinate phosphoribosyltransferase	1.20	-0.32
CCDC75	NM_174931	coiled-coil domain containing 75	1.20	-0.29
NPTXR	NM_014293	neuronal pentraxin receptor	1.19	-0.63
RHOB	NM_004040	ras homolog gene family, member B	1.19	-0.48
CDH7	NM_004361	cadherin 7, type 2	1.17	-0.34
COL5A1	AK057231	collagen, type V, alpha 1	1.17	-0.50
SGMS2	NM_152621	sphingomyelin synthase 2	1.16	-0.32
LOC643802	XM_001716860	similar to M-phase phosphoprotein 10 (U3 small nucleolar ribonucleoprotein)	1.15	-0.53

BCL11A	NM_018014	B-cell CLL/lymphoma 11A (zinc finger protein)	1.14	-0.28
GEN1	NM_182625	Gen homolog 1, endonuclease (Drosophila)	1.14	-0.28
ZP1	NM_207341	zona pellucida glycoprotein 1 (sperm receptor)	1.12	-0.30
EFTUD1	NM_024580	elongation factor Tu GTP binding domain containing 1	1.12	-0.47
REEP6	NM_138393	receptor accessory protein 6	1.10	-0.58
UBA2	NM_005499	ubiquitin-like modifier activating enzyme 2	1.08	-0.38
BRIP1	NM_032043	BRCA1 interacting protein C-terminal helicase 1	1.06	-0.27
KPTN	NM_007059	kaptin (actin binding protein)	1.06	-0.57
DZIP1	NM_014934	DAZ interacting protein 1	1.04	-0.35
MGC16275	NR_026914	hypothetical protein MGC16275	1.04	-0.29
APTX	NM_017692	aprataxin	1.03	-0.29
P2RX4	NM_002560	purinergic receptor P2X, ligand-gated ion channel, 4	1.02	-0.29
PCDH24	NM_017675	protocadherin 24	1.00	-0.37

Overall, ten putative candidates for miR-133a target genes were selected with these data combined. Next, the expression of these molecules was reduced using siRNA-induced gene knockdown system to investigate whether these candidates are functionally important targets of miR-133a in osteosarcoma cells. As a result, knockdown of four candidates (*ANXA2, DUSP11, MAST4*, and *ROD1*) in CD133^{low} SaOS2 cells enhanced drug resistance (**Fig. 37**), and knockdown of five candidates (*ANXA2, DUSP11, SGMS2, SNX30*, and *UBA2*) enhanced invasiveness of CD133^{low} SaOS2 cells (**Fig. 38**).

Of course, the effect of knockdown of these putative target genes would be similar to the effect exerted by miR-133a on these same genes, resulting in enhanced drug resistance and enhanced invasiveness of CD133^{low} SaOS2 cells. Conversely, silencing of miR-133a in CD133^{low} SaOS2 cells would be expected to be permissive for expression of the putative target genes, thereby reducing drug resistance and reducing invasiveness of CD133^{low} SaOS2 cells.

To validate whether these molecules are regulated by miR-133a, the 3'UTR (untranslated region) fragment containing putative miR-133a binding sites was cloned downstream of a luciferase coding sequence, and the luciferase reporter and miR-133a oligonucleotides were co-transfected into SaOS2 cells. As a control, the luciferase reporter and NC oligonucleotides were co-transfected into SaOS2 cells. Luciferase activities were reduced by approximately 39-73% in the cells co-transfected with miR-133a compared with the cells co-transfected with the NC oligonucleotides (**Fig. 39**). From results of this assay, *ANXA2*, *DUSP11*, *MAST4*, *SGMS2*, *SNX30*, and *UBA2* were found to function as direct targets of miR-133a.

Indeed, these target genes or their family genes were previously suggested to function as tumor suppressors in certain other cancers. Gostissa, M et al. (1999) *EMBO J.* 18:6462-71; Caprara, G et al. (2009) *J. Cell. Mol. Med.* 13:2158-70; Nguyen, LN et al. (2006) *Clin. Cancer Res.* 12:6952-9. *ANXA2* has been reported to be associated with tumor-suppressive function in osteosarcoma (Gillette, JM (2004) *J. Cell Biochem.* 92:820-32), whereas *MAST4* has been unknown in tumor biology (Garland, P (2008) *Brain Res.* 21:12-19).

Indeed, as disclosed by the present invention, the expression of all these targets was increased by silencing of miR-133a in CD133^{high} cells (**Fig. 40**) and decreased by miR-133a upregulation in CD133^{low} cells (**Fig. 41**), consistent with observed inverse correlations with the expression of CD133 and miR-133a in both xenografted tumors (**Fig. 42**) and clinical samples (results not shown). The increased expression of the targets by silencing of miR-133a was confirmed by qRT-PCR (results not shown) and immunohistochemistry of LNA-treated tumors (results not shown). Finally, in investigating the relationships between the expression of these targets and osteosarcoma patient prognosis, a strikingly close correlation was found between the mRNA expression of the miR-133a targets and patient prognosis (**Fig. 43**). Patients with higher expression levels of these targets survived much longer than patients with lower expression, indicating that these targets could function as novel tumor-suppressors in osteosarcoma.

CLAIMS

We claim:

1. A method of treating osteosarcoma, comprising administering to a subject in need thereof an effective amount of an antisense molecule specific for a microRNA (miRNA) selected from miR-1, miR-10b, and miR-133a.

2. The method of claim 1, wherein the antisense molecule is stabilized RNA.

3. The method of claim 2, wherein the stabilized RNA is a locked nucleic acid (LNA) oligonucleotide.

4. The method of claim 1, wherein the antisense molecule is DNA.

5. The method of claim 1, wherein the antisense molecule is 20-30 nucleotides long and comprises a nucleotide sequence at least 90 percent identical to
5′-ACATACTTCTTTACATTCCA-3′ (SEQ ID NO:4),
5′-ACAAATTCGGTTCTACAGGGT-3′ (SEQ ID NO:5), or
5′-CAGCTGGTTGAAGGGGACCAA-3′ (SEQ ID NO:6).

6. The method of claim 5, wherein the antisense molecule is 21-30 nucleotides long and comprises a nucleotide sequence at least 95 percent identical to
5′-ACATACTTCTTTACATTCCA-3′ (SEQ ID NO:4),
5′-ACAAATTCGGTTCTACAGGGT-3′ (SEQ ID NO:5), or
5′-CAGCTGGTTGAAGGGGACCAA-3′ (SEQ ID NO:6).

7. The method of claim 6, wherein the sequence of the antisense molecule is
5′-ACATACTTCTTTACATTCCA-3′ (SEQ ID NO:4),
5′-ACAAATTCGGTTCTACAGGGT-3′ (SEQ ID NO:5), or
5′-CAGCTGGTTGAAGGGGACCAA-3′ (SEQ ID NO:6).

8. The method of claim 1, wherein the antisense molecule is 20-30 nucleotides long and comprises a nucleotide sequence at least 90 percent identical to
5′-AUACAUACUUCUUUACAUUCCA-3′ (SEQ ID NO:7),
5′-CACAAAUUCGGUUCUACAGGGUA-3′ (SEQ ID NO:8),
5′-CAGCUGGUUGAAGGGGACCAAA-3′ (SEQ ID NO:9),
5′-ATACATACTTCTTTACATTCCA-3′ (SEQ ID NO:10),

5′-CACAAATTCGGTTCTACAGGGTA-3′ (SEQ ID NO:11), or
5′-CAGCTGGTTGAAGGGGACCAAA-3′ (SEQ ID NO:12).

9. The method of claim 8, wherein the antisense molecule is 21-30 nucleotides long and comprises a nucleotide sequence at least 95 percent identical to
5′-AUACAUACUUCUUUACAUUCCA-3′ (SEQ ID NO:7),
5′-CACAAAUUCGGUUCUACAGGGUA-3′ (SEQ ID NO:8),
5′-CAGCUGGUUGAAGGGGACCAAA-3′ (SEQ ID NO:9),
5′-ATACATACTTCTTTACATTCCA-3′ (SEQ ID NO:10),
5′-CACAAATTCGGTTCTACAGGGTA-3′ (SEQ ID NO:11), or
5′-CAGCTGGTTGAAGGGGACCAAA-3′ (SEQ ID NO:12).

10. The method of claim 9, wherein the sequence of the antisense molecule is
5′-AUACAUACUUCUUUACAUUCCA-3′ (SEQ ID NO:7),
5′-CACAAAUUCGGUUCUACAGGGUA-3′ (SEQ ID NO:8),
5′-CAGCUGGUUGAAGGGGACCAAA-3′ (SEQ ID NO:9),
5′-ATACATACTTCTTTACATTCCA-3′ (SEQ ID NO:10),
5′-CACAAATTCGGTTCTACAGGGTA-3′ (SEQ ID NO:11), or
5′-CAGCTGGTTGAAGGGGACCAAA-3′ (SEQ ID NO:12).

11. The method of any one of claims 1-10, wherein the antisense molecule is associated with a nucleic acid delivery vehicle.

12. The method of any one of claims 1-11, wherein the osteosarcoma is metastatic osteosarcoma.

13. An isolated nucleic acid molecule 20-30 nucleotides long comprising a nucleotide sequence at least 90 percent identical to 5′-ACATACTTCTTTACATTCCA-3′ (SEQ ID NO:4), 5′-ACAAATTCGGTTCTACAGGGT-3′ (SEQ ID NO:5), or
5′-CAGCTGGTTGAAGGGGACCAA-3′ (SEQ ID NO:6).

14. The isolated nucleic acid molecule of claim 13, wherein the isolated nucleic acid molecule is 21-30 nucleotides long and comprises a nucleotide sequence at least 95 percent identical to 5′-ACATACTTCTTTACATTCCA-3′ (SEQ ID NO:4),
5′-ACAAATTCGGTTCTACAGGGT-3′ (SEQ ID NO:5), or
5′-CAGCTGGTTGAAGGGGACCAA-3′ (SEQ ID NO:6).

15. The isolated nucleic acid molecule of claim 14, wherein the sequence of the isolated nucleic acid molecule is 5′-ACATACTTCTTTACATTCCA-3′ (SEQ ID NO:4), 5′-ACAAATTCGGTTCTACAGGGT-3′ (SEQ ID NO:5), or 5′-CAGCTGGTTGAAGGGGACCAA-3′ (SEQ ID NO:6).

16. An isolated nucleic acid molecule 20-30 nucleotides long comprising a nucleotide sequence at least 90 percent identical to 5′-AUACAUACUUCUUUACAUUCCA-3′ (SEQ ID NO:7), 5′-CACAAAUUCGGUUCUACAGGGUA-3′ (SEQ ID NO:8), 5′-CAGCUGGUUGAAGGGGACCAAA-3′ (SEQ ID NO:9), 5′-ATACATACTTCTTTACATTCCA-3′ (SEQ ID NO:10), 5′-CACAAATTCGGTTCTACAGGGTA-3′ (SEQ ID NO:11), or 5′-CAGCTGGTTGAAGGGGACCAAA-3′ (SEQ ID NO:12).

17. The isolated nucleic acid molecule of claim 16, wherein the isolated nucleic acid molecule is 21-30 nucleotides long and comprises a nucleotide sequence at least 95 percent identical to 5′-AUACAUACUUCUUUACAUUCCA-3′ (SEQ ID NO:7), 5′-CACAAAUUCGGUUCUACAGGGUA-3′ (SEQ ID NO:8), 5′-CAGCUGGUUGAAGGGGACCAAA-3′ (SEQ ID NO:9), 5′-ATACATACTTCTTTACATTCCA-3′ (SEQ ID NO:10), 5′-CACAAATTCGGTTCTACAGGGTA-3′ (SEQ ID NO:11), or 5′-CAGCTGGTTGAAGGGGACCAAA-3′ (SEQ ID NO:12).

18. The isolated nucleic acid molecule of claim 17, wherein the sequence of the isolated nucleic acid molecule is 5′-AUACAUACUUCUUUACAUUCCA-3′ (SEQ ID NO:7), 5′-CACAAAUUCGGUUCUACAGGGUA-3′ (SEQ ID NO:8), 5′-CAGCUGGUUGAAGGGGACCAAA-3′ (SEQ ID NO:9), 5′-ATACATACTTCTTTACATTCCA-3′ (SEQ ID NO:10), 5′-CACAAATTCGGTTCTACAGGGTA-3′ (SEQ ID NO:11), or 5′-CAGCTGGTTGAAGGGGACCAAA-3′ (SEQ ID NO:12).

19. The isolated nucleic acid molecule of any one of claims 13-18, wherein the nucleic acid molecule is associated with a nucleic acid delivery vehicle.

20. A method of assessing resistance of osteosarcoma to an anti-cancer therapy, comprising:

obtaining a tissue sample comprising osteosarcoma cells;

isolating from the sample cells expressing CD133;

measuring a first level of expression by the CD133-expressing cells of at least one microRNA (miRNA) selected from the group consisting of miR-1, miR-10b, and miR-133a;

contacting the CD133-expressing cells with an anti-cancer therapy; and

measuring a second level of expression by the CD133-expressing cells of the at least one miRNA, wherein a second level of expression greater than the first level of expression indicates the osteosarcoma is resistant to the anti-cancer therapy.

21. The method of claim 20, wherein the anti-cancer therapy is selected from the group consisting of cisplatin, doxorubicin, methotrexate, and any combination thereof.

22. A method of screening for osteosarcoma, comprising:

performing on a tissue sample from a subject an assay specifically capable of detecting at least one microRNA (miRNA) selected from the group consisting of miR-1, miR-10b, and miR-133a, wherein detection by the assay of the presence in the sample of the at least one miRNA indicates the subject is at risk of having osteosarcoma.

23. The method of claim 22, wherein the tissue is blood.

24. The method of claim 22, wherein the tissue is serum.

25. A method of monitoring osteosarcoma, comprising:

(a) performing, on a tissue sample obtained from a subject having osteosarcoma or having been treated for osteosarcoma, an assay specifically capable of quantifying the level of expression of at least one microRNA (miRNA) selected from the group consisting of miR-1, miR-10b, and miR-133a; and

(b) repeating step (a) on a later-obtained tissue sample from the subject, wherein a level of expression of the at least one miRNA in the later-obtained sample greater than the level of expression of the at least one miRNA in the earlier-obtained sample indicates the osteosarcoma is progressive, and a level of expression of the at least one miRNA in the later-obtained sample lesser than the level of expression of the at least one miRNA in the earlier-obtained sample indicates the osteosarcoma is regressive.

26. The method of claim 25, wherein the tissue is blood.

27. The method of claim 25, wherein the tissue is serum.

Fig. 1

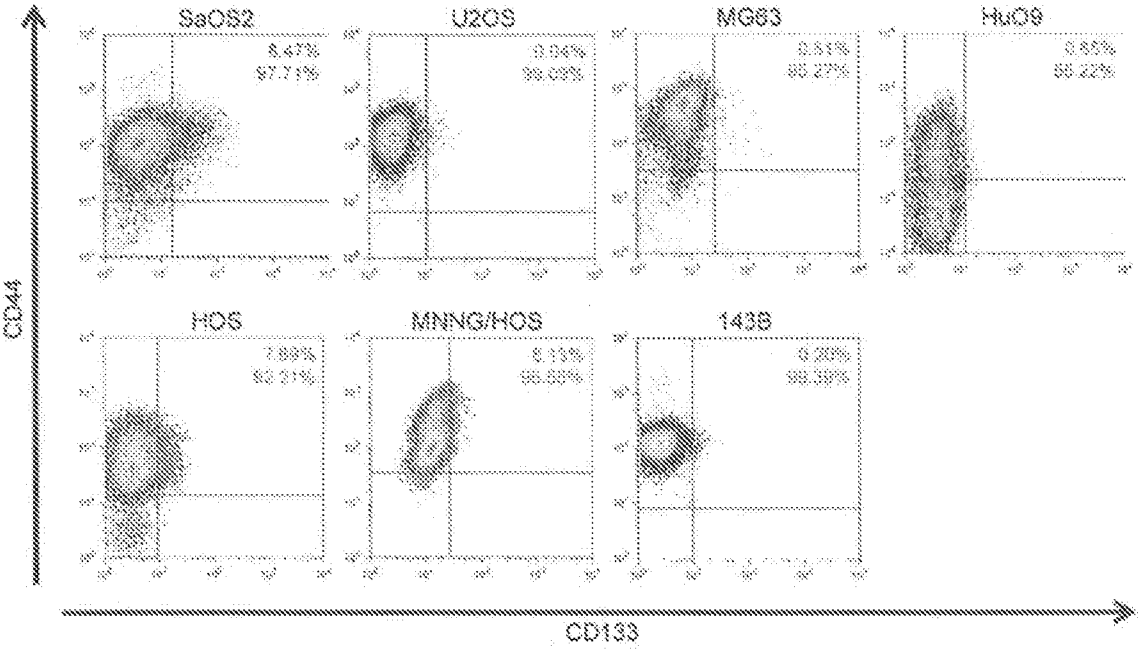
SaOS2
8.47%
97.71%
U2OS
0.04%
98.09%
MG63
0.51%
96.27%
HuO9
0.85%
98.22%
HOS
7.89%
93.31%
MNNG/HOS
0.13%
98.80%
143B
0.20%
98.39%
CD44
CD133

Fig. 2

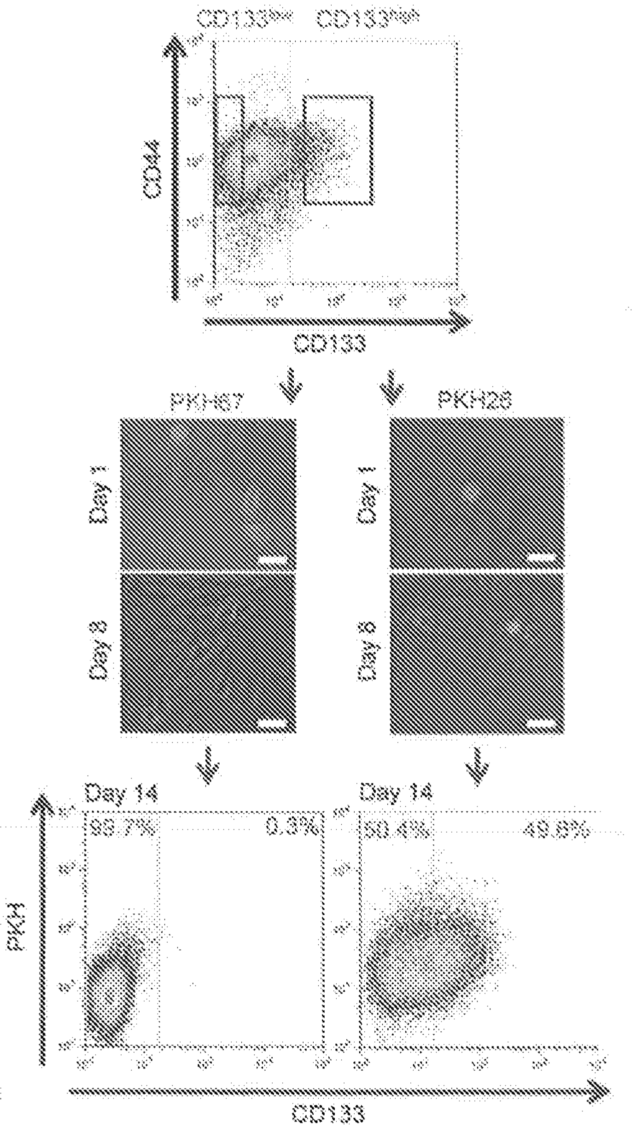
CD133^{low}
CD133^{high}
CD44
CD133
PKH67
PKH26
Day 1
Day 8
Day 1
Day 8
Day 14
99.7%
0.3%
Day 14
50.4%
49.6%
PKH
CD133

Fig. 3

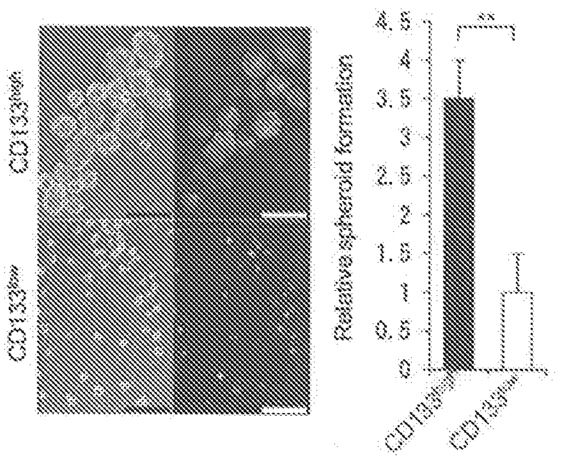
CD133^high
CD133^low
Relative spheroid formation
4.5
4
3.5
3
2.5
2
1.5
1
0.5
0
**
CD133^high
CD133^low

Fig. 4

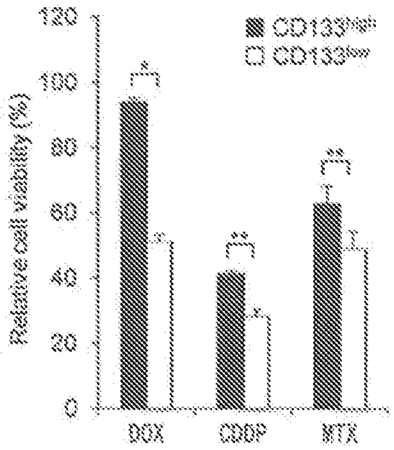
CD133^{high}
CD133^{low}
Relative cell viability (%)
120
100
80
60
40
20
0
*
**
**
DOX
CDDP
MTX

Fig. 5

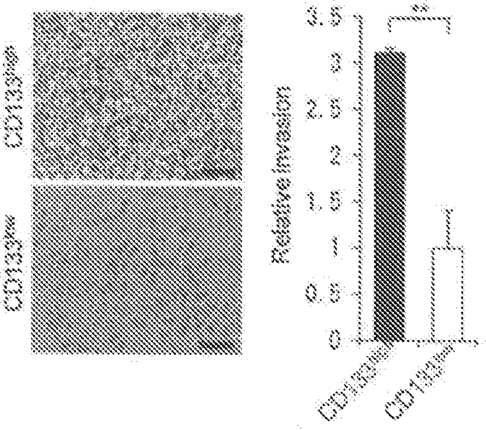
CD133high
CD133low
Relative Invasion
3.5
3
2.5
2
1.5
1
0.5
0
**
CD133high
CD133low

Fig. 6

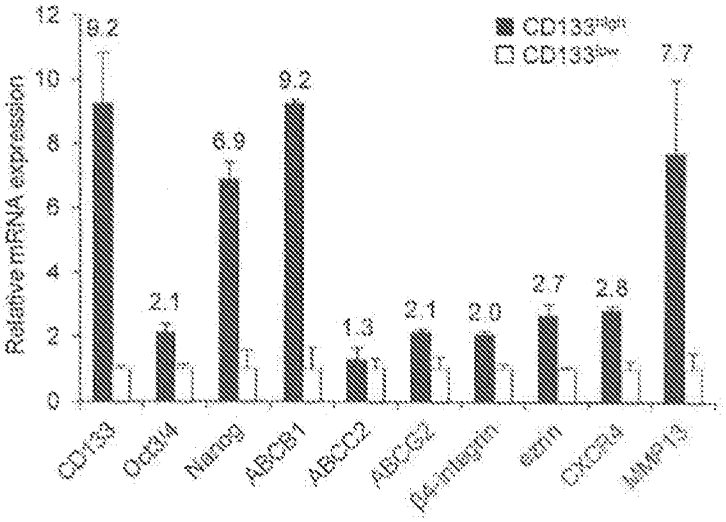
Relative mRNA expression
0
2
4
6
8
10
12
$CD133^{High}$
$CD133^{low}$
9.2
2.1
6.9
9.2
1.3
2.1
2.0
2.7
2.8
7.7
CD133
Oct3/4
Nanog
ABCB1
ABCC2
ABCG2
β6-integrin
ezrin
CXCR4
MMP13

Fig. 7

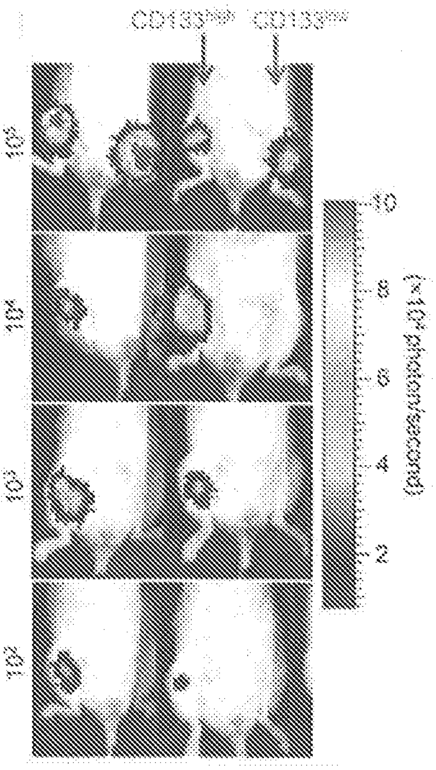
CD133high
CD133low
10^5
10^4
10^3
10^2
10
8
6
4
2
(×10^4 photon/second)

Fig. 8

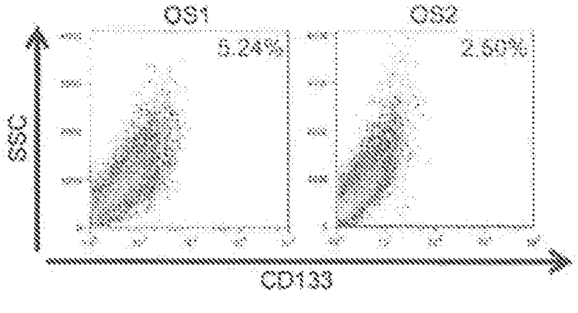

Fig. 9

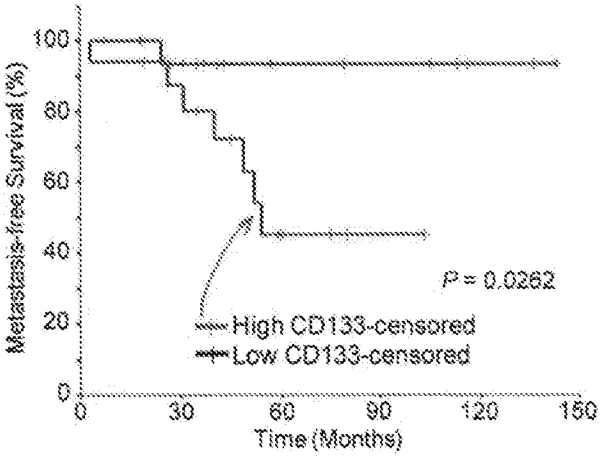
Metastasis-free Survival (%)
100
80
60
40
20
0
0
30
60
90
120
150
Time (Months)
P = 0.0262
High CD133-censored
Low CD133-censored

Fig. 10

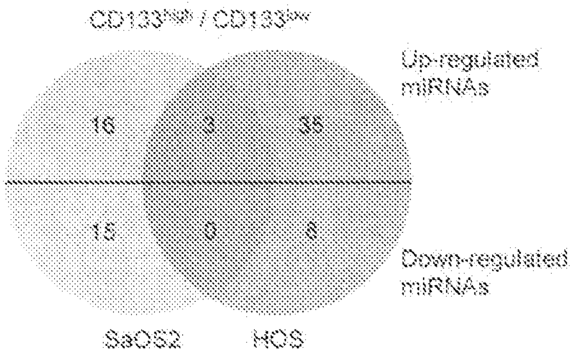
$CD133^{high}$ / $CD133^{low}$
Up-regulated miRNAs
16
3
35
15
0
8
Down-regulated miRNAs
SaOS2
HOS

Fig. 11

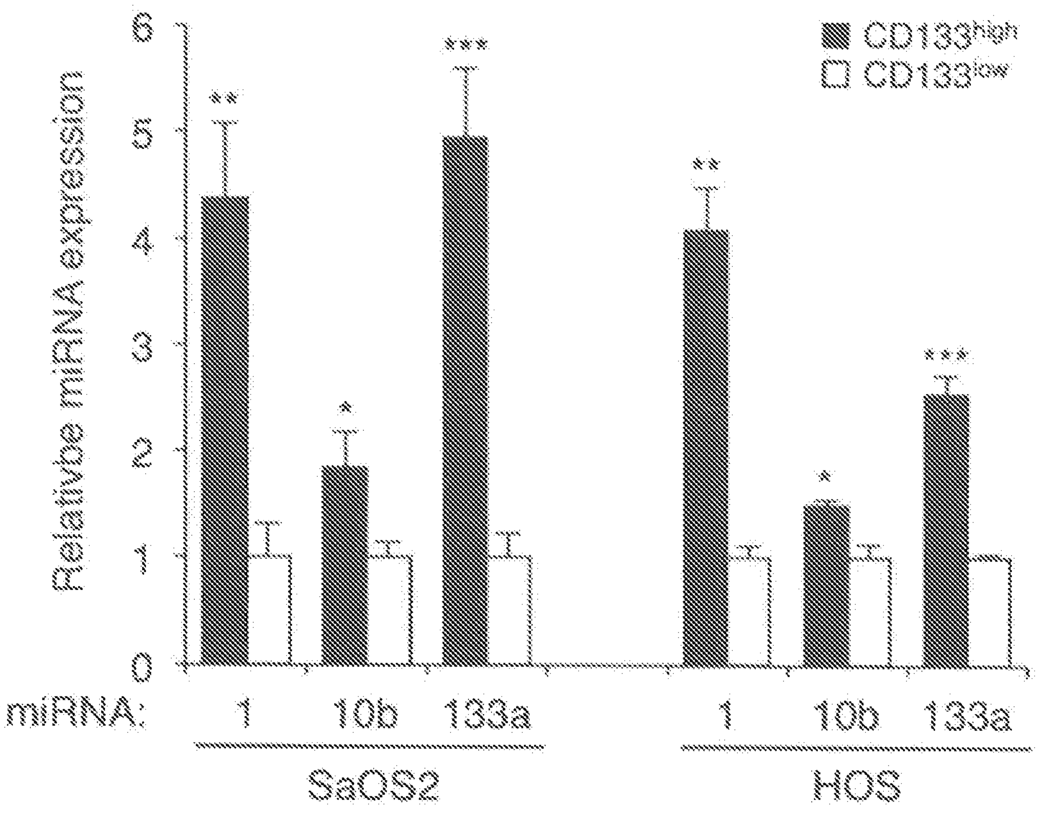
CD133^high
CD133^low
Relativbe miRNA expression
0
1
2
3
4
5
6
**
*
***
**
*
***
miRNA:
1
10b
133a
1
10b
133a
SaOS2
HOS

Fig. 12

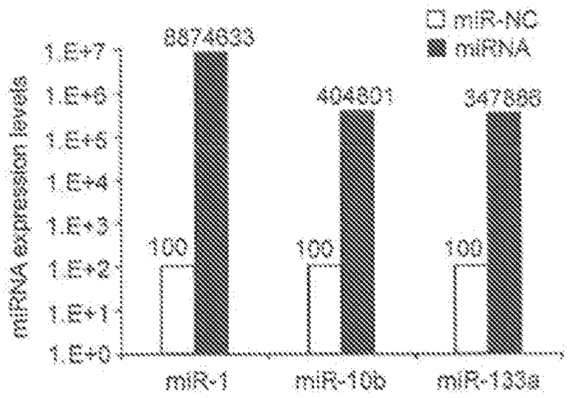
☐ miR-NC
▨ miRNA
miRNA expression levels
1.E+7
1.E+6
1.E+5
1.E+4
1.E+3
1.E+2
1.E+1
1.E+0
8874633
404801
347888
100
100
100
miR-1
miR-10b
miR-133a

Fig. 13

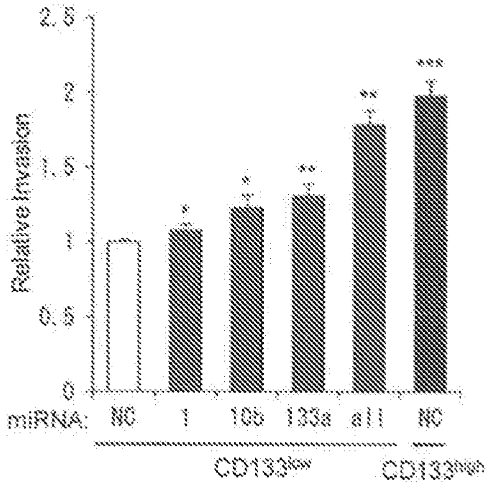
Relative invasion
2.5
2
1.5
1
0.5
0
*
*
**
**
***
miRNA:
NC
1
10b
133a
all
NC
$CD133^{low}$
$CD133^{high}$

Fig. 14

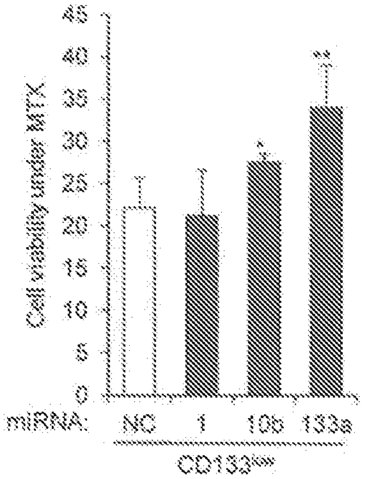
Cell viability under MTX
45
40
35
30
25
20
15
10
5
0
**
*
miRNA:
NC
1
10b
133a
CD133^{low}

Fig. 15

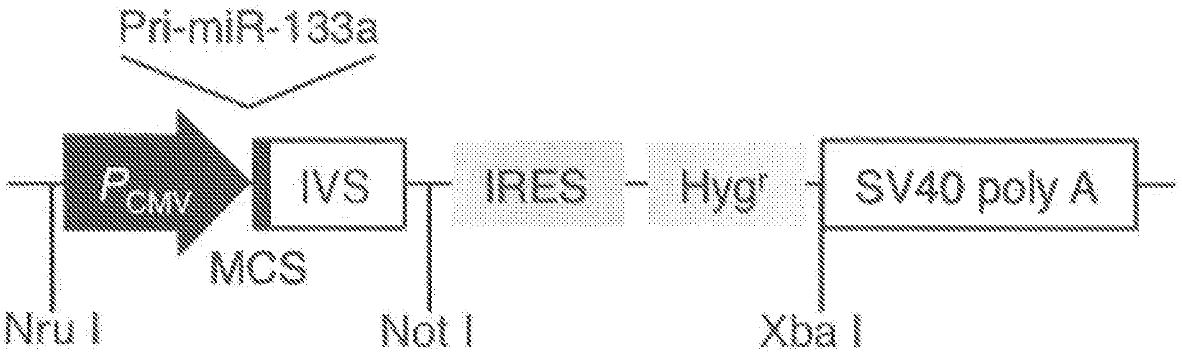

Fig. 16

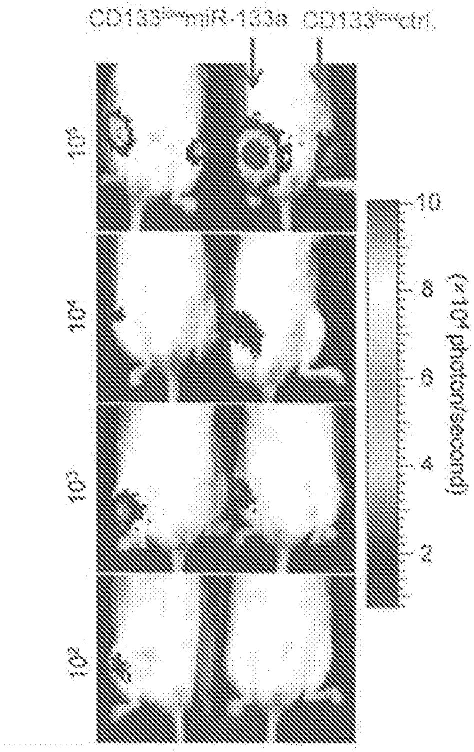
CD133^low miR-133a
CD133^low ctrl.
10^5
10^4
10^3
10^2
10
8
6
4
2
(×10^4 photon/second)

Fig. 17

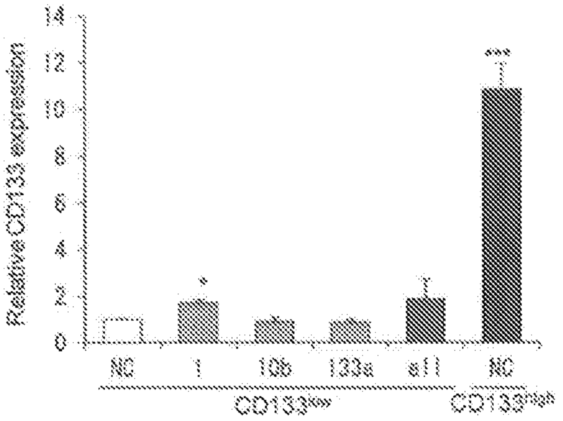
Relative CD133 expression
0
2
4
6
8
10
12
14
*
***
NC
1
10b
133a
all
NC
CD133low
CD133high

Fig. 18

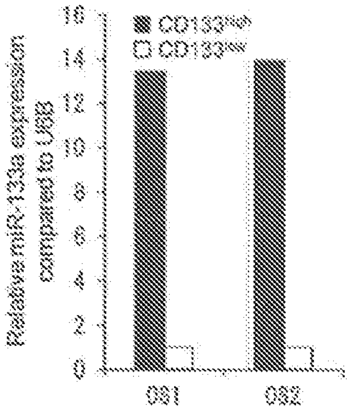
Relative miR-133a expression compared to U6B
16
14
12
10
8
6
4
2
0
▨ CD133^high
☐ CD133^low
OS1
OS2

Fig. 19

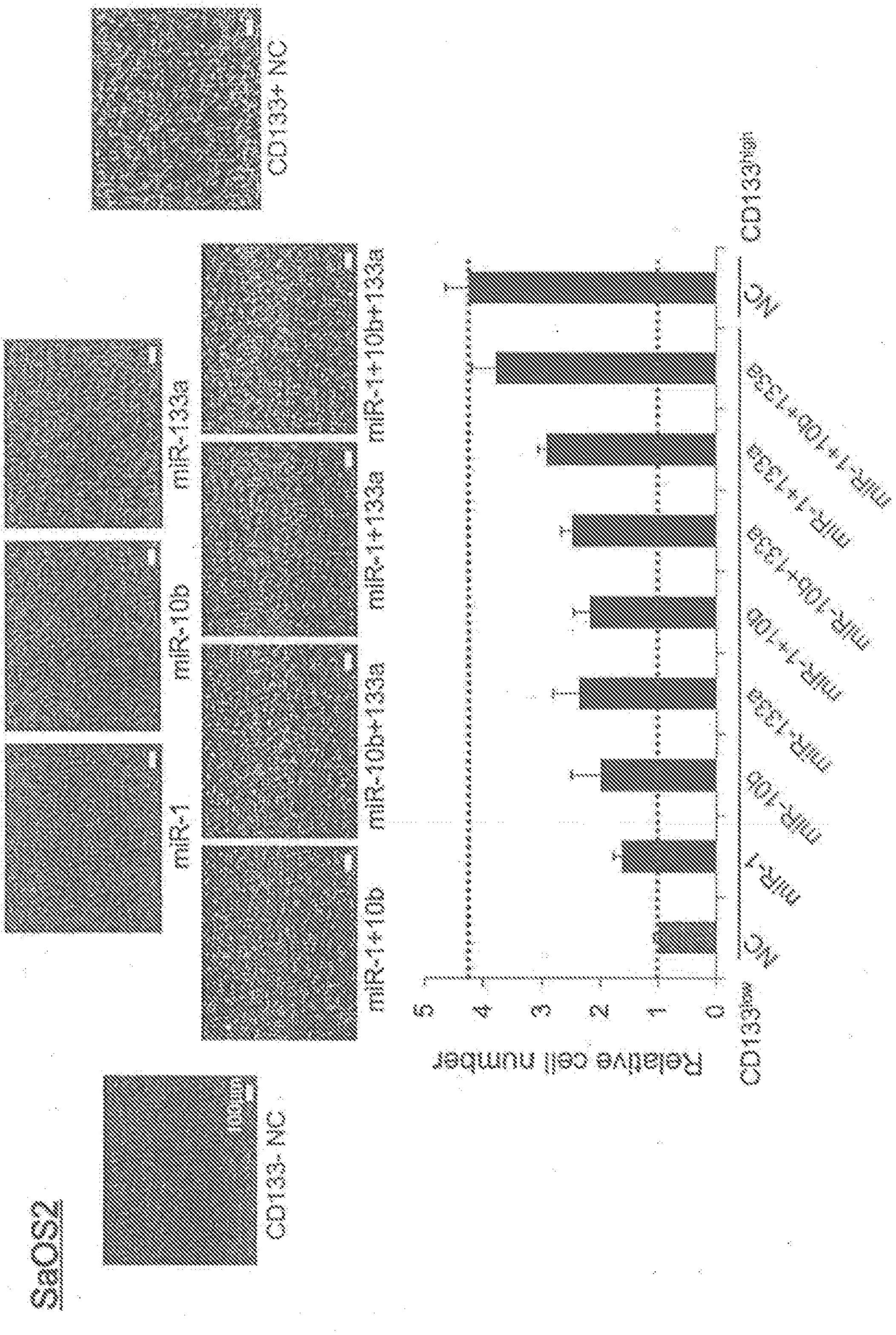
SaOS2
CD133- NC
100μm
miR-1
miR-10b
miR-133a
CD133+ NC
miR-1+10b
miR-10b+133a
miR-1+133a
miR-1+10b+133a
Relative cell number
0
1
2
3
4
5
NC
miR-1
miR-10b
miR-133a
miR-1+10b
miR-10b+133a
miR-1+133a
miR-1+10b+133a
NC
CD133^{low}
CD133^{high}

Fig. 20

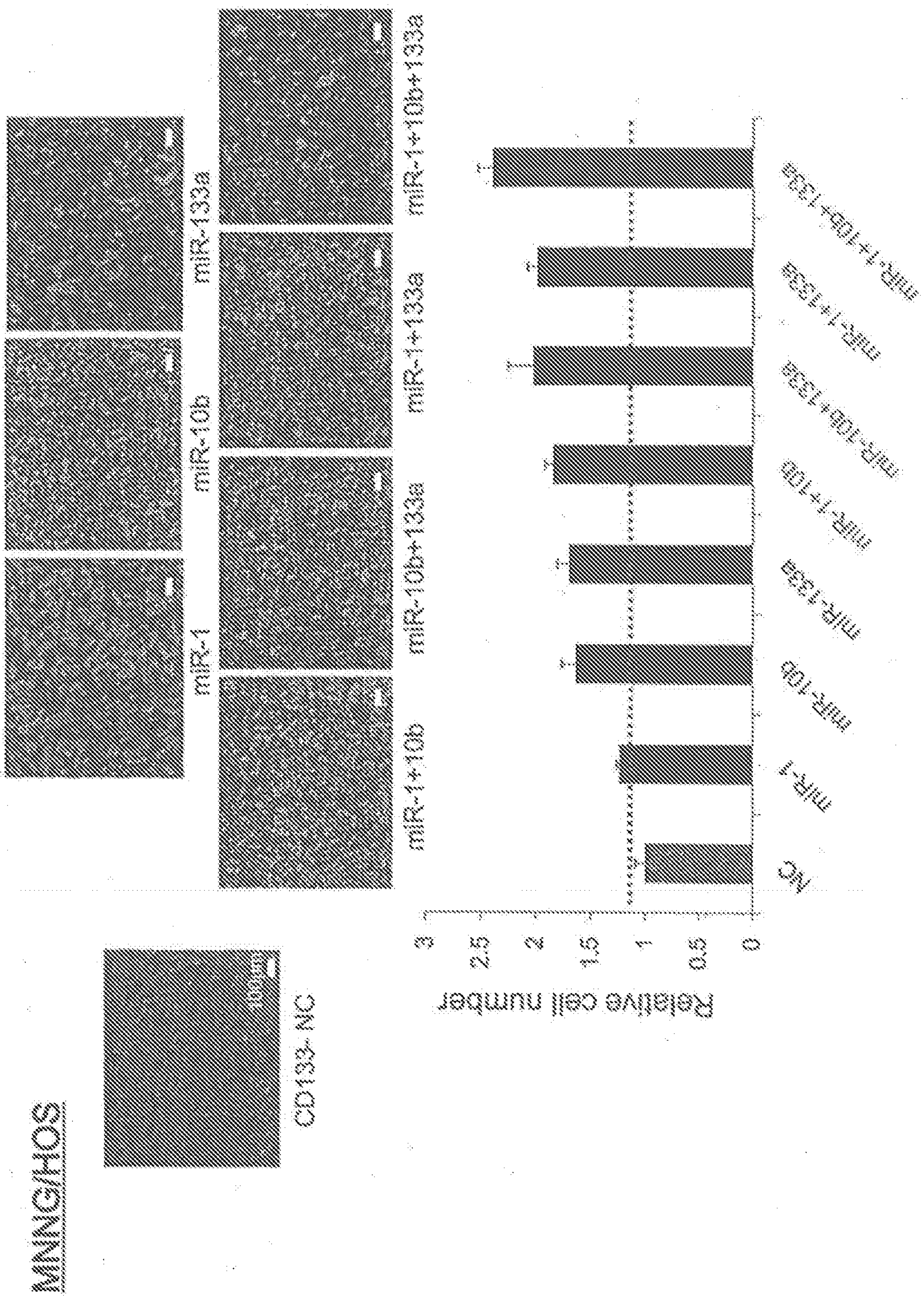
MNNG/HOS
CD133- NC
100μm
miR-1
miR-10b
miR-133a
miR-1+10b
miR-10b+133a
miR-1+133a
miR-1+10b+133a
Relative cell number
3
2.5
2
1.5
1
0.5
0
NC
miR-1
miR-10b
miR-133a
miR-1+10b
miR-10b+133a
miR-1+133a
miR-1+10b+133a

Fig. 21

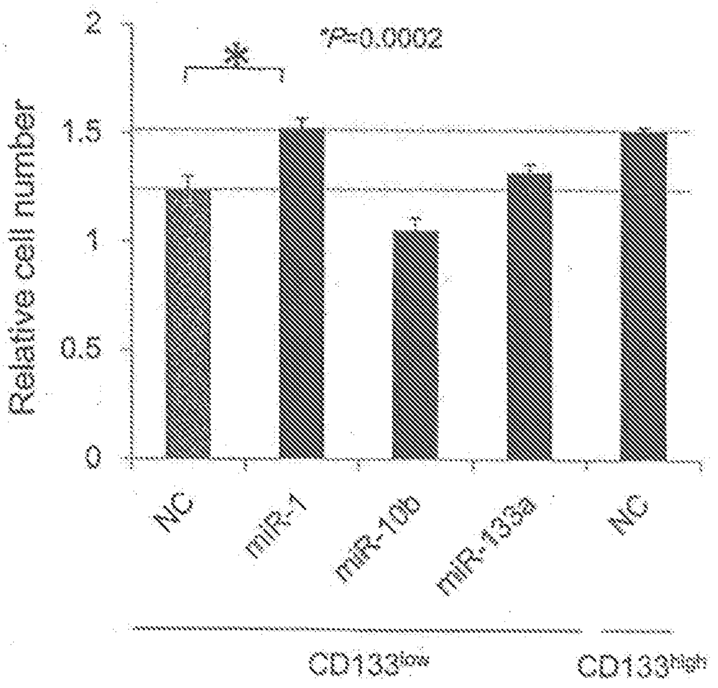
Relative cell number
2
1.5
1
0.5
0
*
*P=0.0002
NC
miR-1
miR-10b
miR-133a
NC
CD133^low
CD133^high

Fig. 22

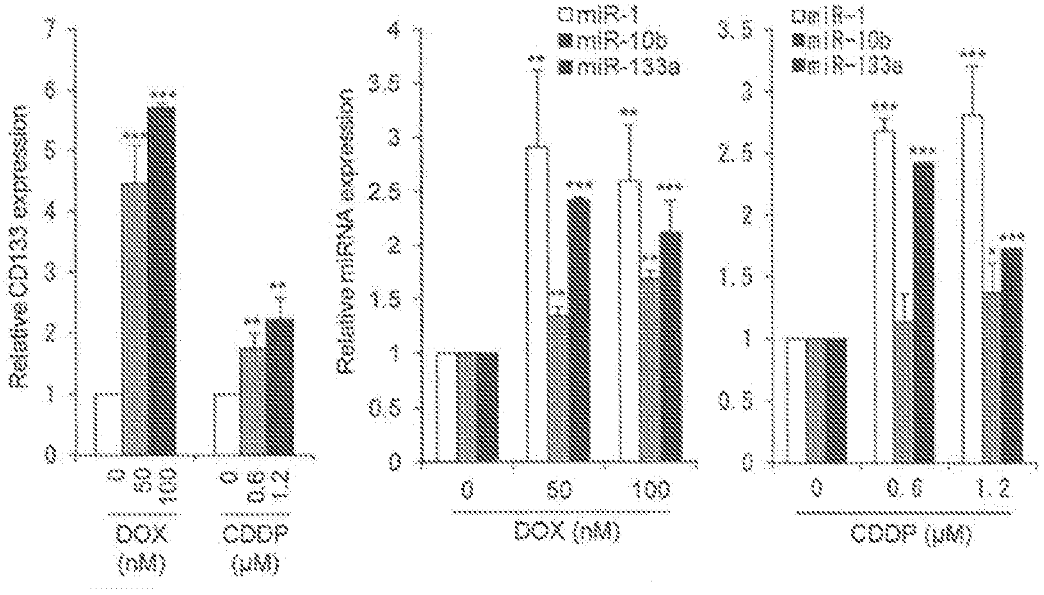
Relative CD133 expression
0
1
2
3
4
5
6
7
0
50
100
DOX (nM)
0
0.6
1.2
CDDP (μM)
Relative miRNA expression
0
0.5
1
1.5
2
2.5
3
3.5
4
miR-1
miR-10b
miR-133a
0
50
100
DOX (nM)
0
0.5
1
1.5
2
2.5
3
3.5
miR-1
miR-10b
miR-133a
0
0.6
1.2
CDDP (μM)

Fig. 23

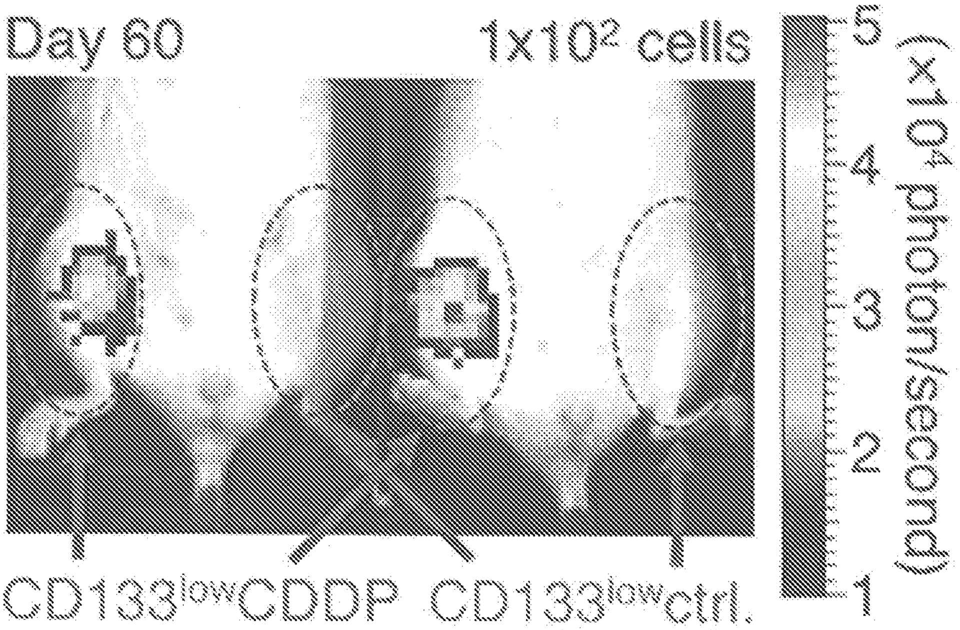
Day 60
1x10² cells
CD133lowCDDP
CD133lowctrl.
5
4
3
2
1
(x10⁴ photon/second)

Fig. 24

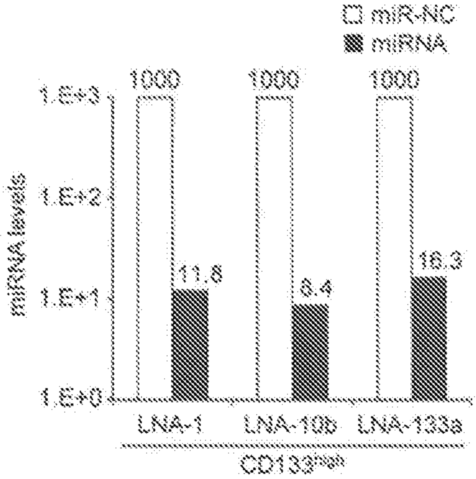
miR-NC
miRNA
miRNA levels
1.E+3
1.E+2
1.E+1
1.E+0
1000
1000
1000
11.8
8.4
16.3
LNA-1
LNA-10b
LNA-133a
CD133high

Fig. 25

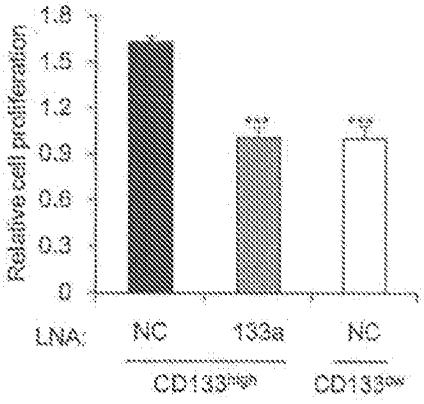
Relative cell proliferation
1.8
1.5
1.2
0.9
0.6
0.3
0
***
***
LNA:
NC
133a
NC
CD133^{high}
CD133^{low}

Fig. 26

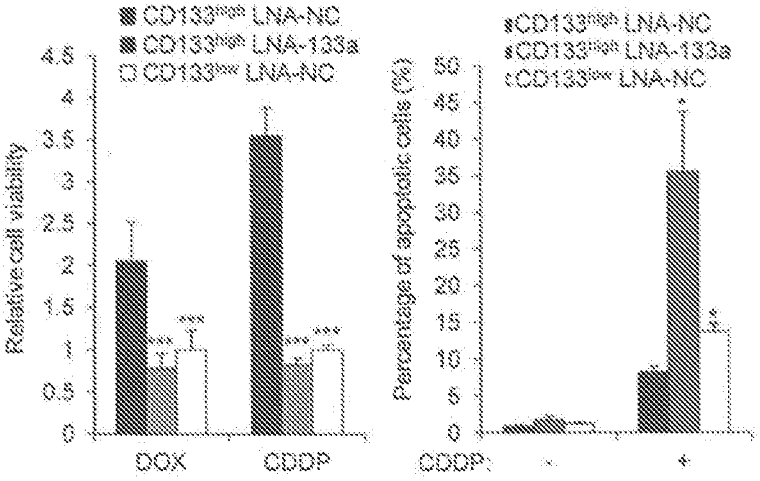
▨ CD133^{high} LNA-NC
▨ CD133^{high} LNA-133a
☐ CD133^{low} LNA-NC
Relative cell viability
4.5
4
3.5
3
2.5
2
1.5
1
0.5
0
***
***
***
***
DOX
CDDP
▨CD133^{high} LNA-NC
▨CD133^{high} LNA-133a
☐CD133^{low} LNA-NC
Percentage of apoptotic cells (%)
50
45
40
35
30
25
20
15
10
5
0
*
*
CDDP:
-
+

Fig. 27

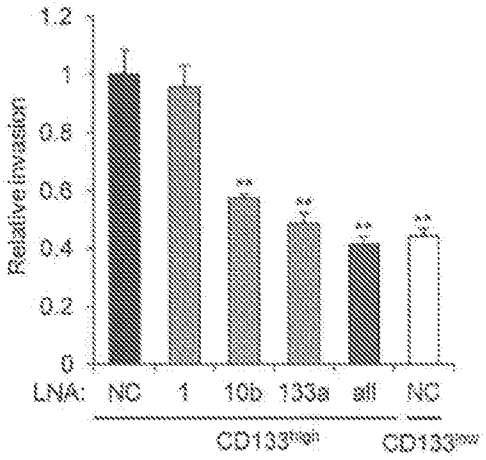
Relative invasion
1.2
1
0.8
0.6
0.4
0.2
0
**
**
**
**
LNA: NC 1 10b 133a all NC
CD133^high
CD133^low

Fig. 28

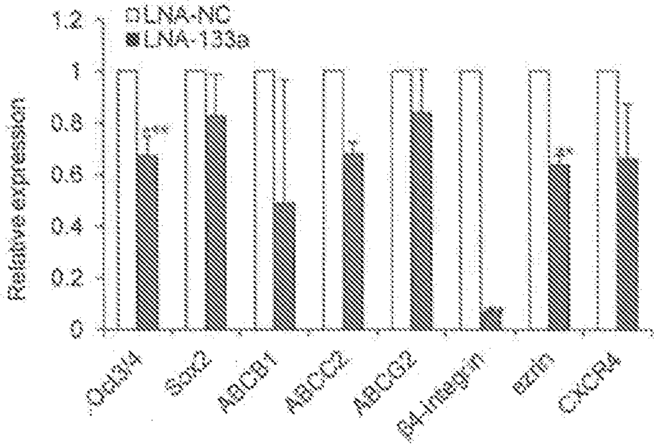
□ LNA-NC
▨ LNA-133a
Relative expression
1.2
1
0.8
0.6
0.4
0.2
0
***
*
**
Oct3/4
Sox2
ABCB1
ABCC2
ABCG2
β4-integrin
ezrin
CXCR4

Fig. 29

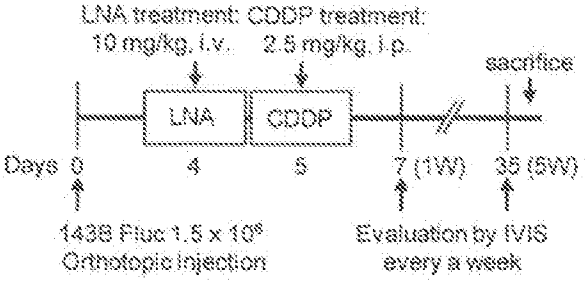
LNA treatment: 10 mg/kg, i.v.
CDDP treatment: 2.5 mg/kg, i.p.
sacrifice
LNA
CDDP
Days 0
4
5
7 (1W)
35 (5W)
1438 Fluc 1.5×10^6 Orthotopic injection
Evaluation by IVIS every a week

Fig. 30

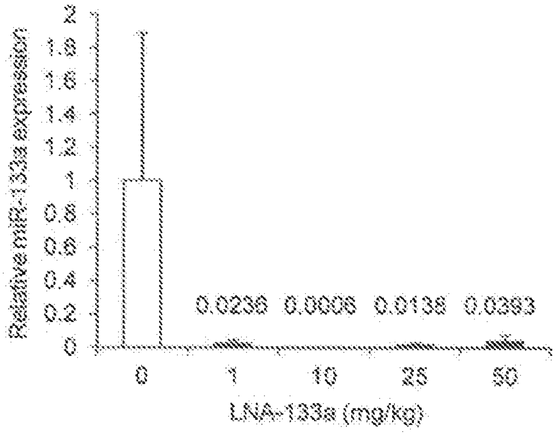
Relative miR-133a expression
2
1.8
1.6
1.4
1.2
1
0.8
0.6
0.4
0.2
0
0.0236
0.0006
0.0136
0.0393
0
1
10
25
50
LNA-133a (mg/kg)

Fig. 31

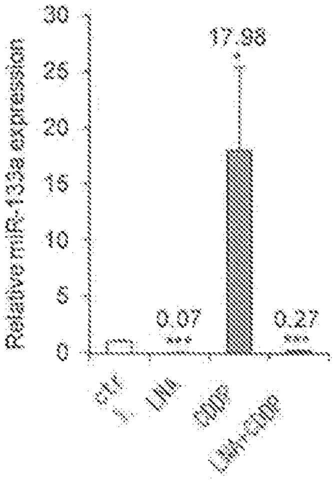
Relative miR-133a expression
30
25
20
15
10
5
0
17.98
*
0.07
***
0.27
***
LNA
CDDP
LNA+CDDP

Fig. 32

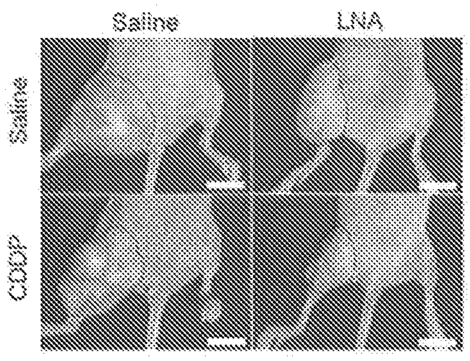

Fig. 33

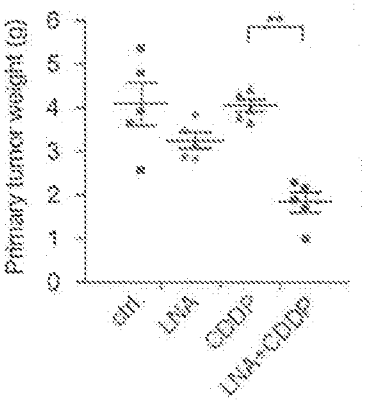

Fig. 34

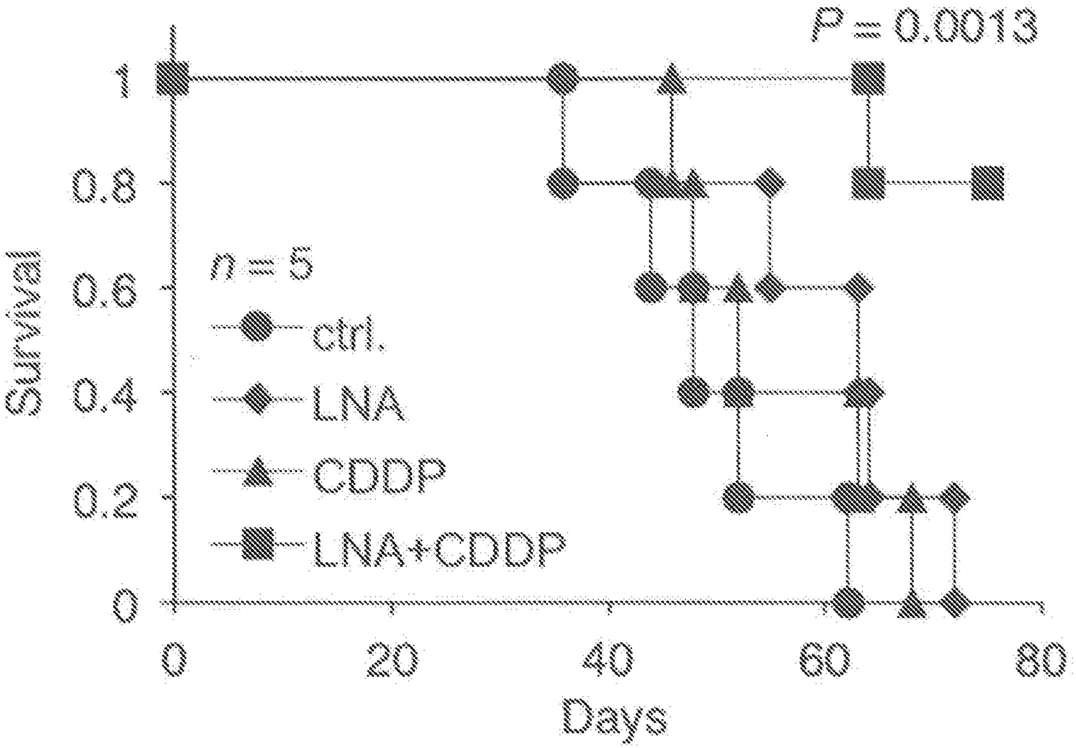
P = 0.0013
1
0.8
0.6
0.4
0.2
0
Survival
n = 5
ctrl.
LNA
CDDP
LNA+CDDP
0
20
40
60
80
Days

Fig. 35

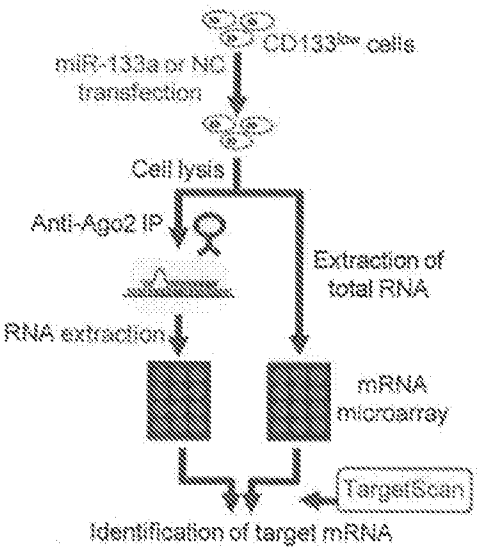
CD133^low cells
miR-133a or NC transfection
Cell lysis
Anti-Ago2 IP
Extraction of total RNA
RNA extraction
mRNA microarray
TargetScan
Identification of target mRNA

Fig. 36

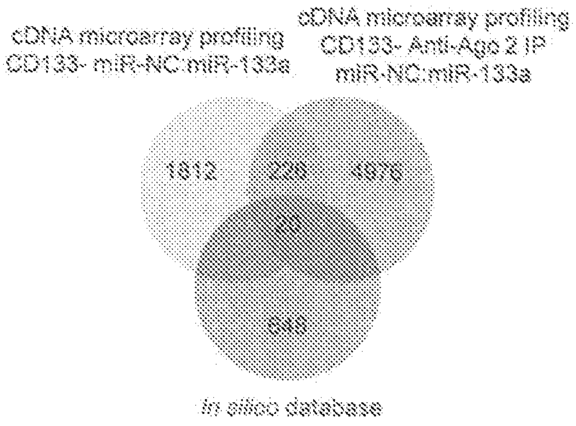
cDNA microarray profiling
CD133- miR-NC:miR-133a
cDNA microarray profiling
CD133- Anti-Ago 2 IP
miR-NC:miR-133a
1812
226
4976
648
In silico database

Fig. 37

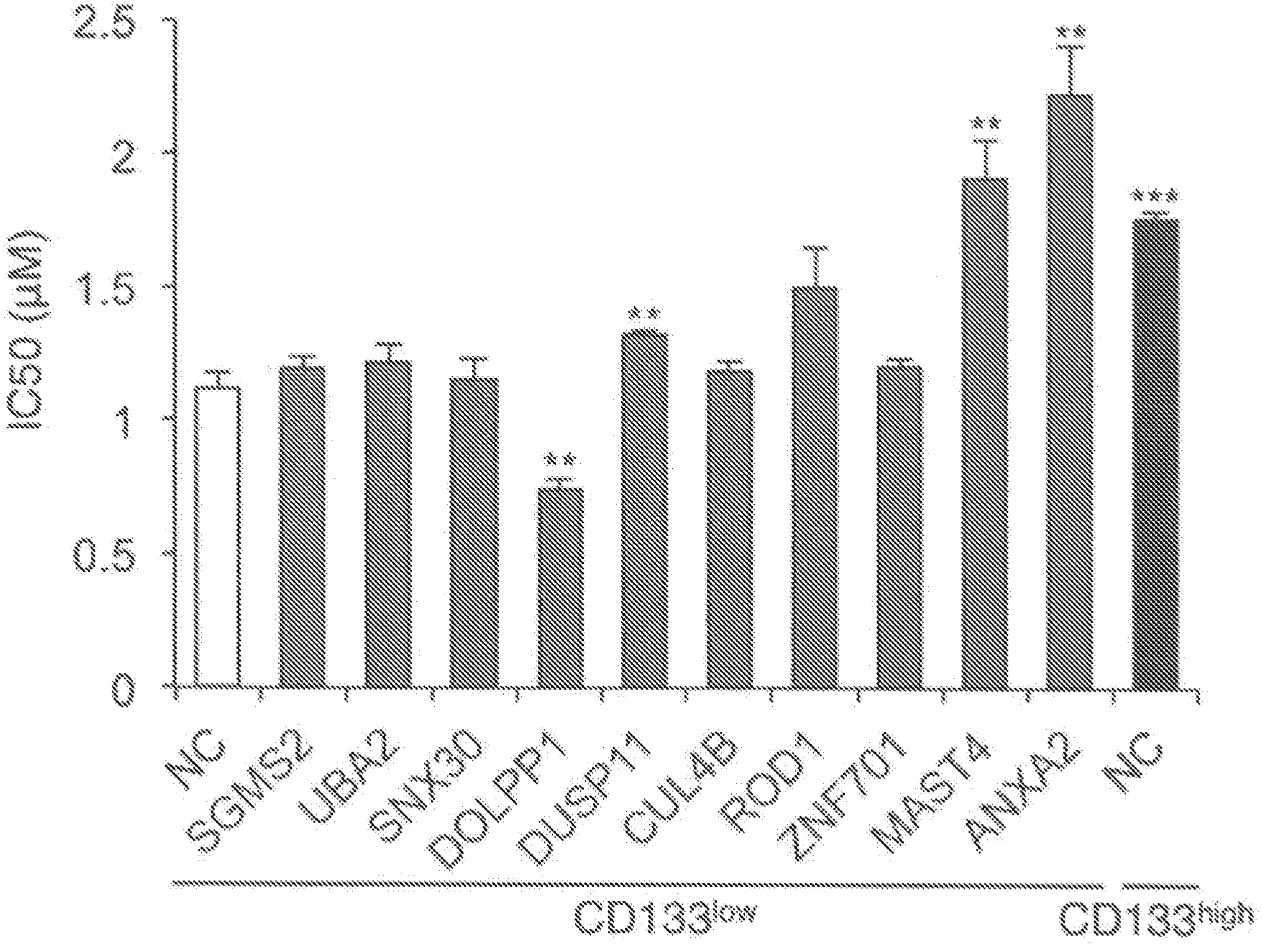
IC50 (μM)
2.5
2
1.5
1
0.5
0
**
**
**
**
***
NC
SGMS2
UBA2
SNX30
DOLPP1
DUSP11
CUL4B
ROD1
ZNF701
MAST4
ANXA2
NC
CD133low
CD133high

Fig. 38

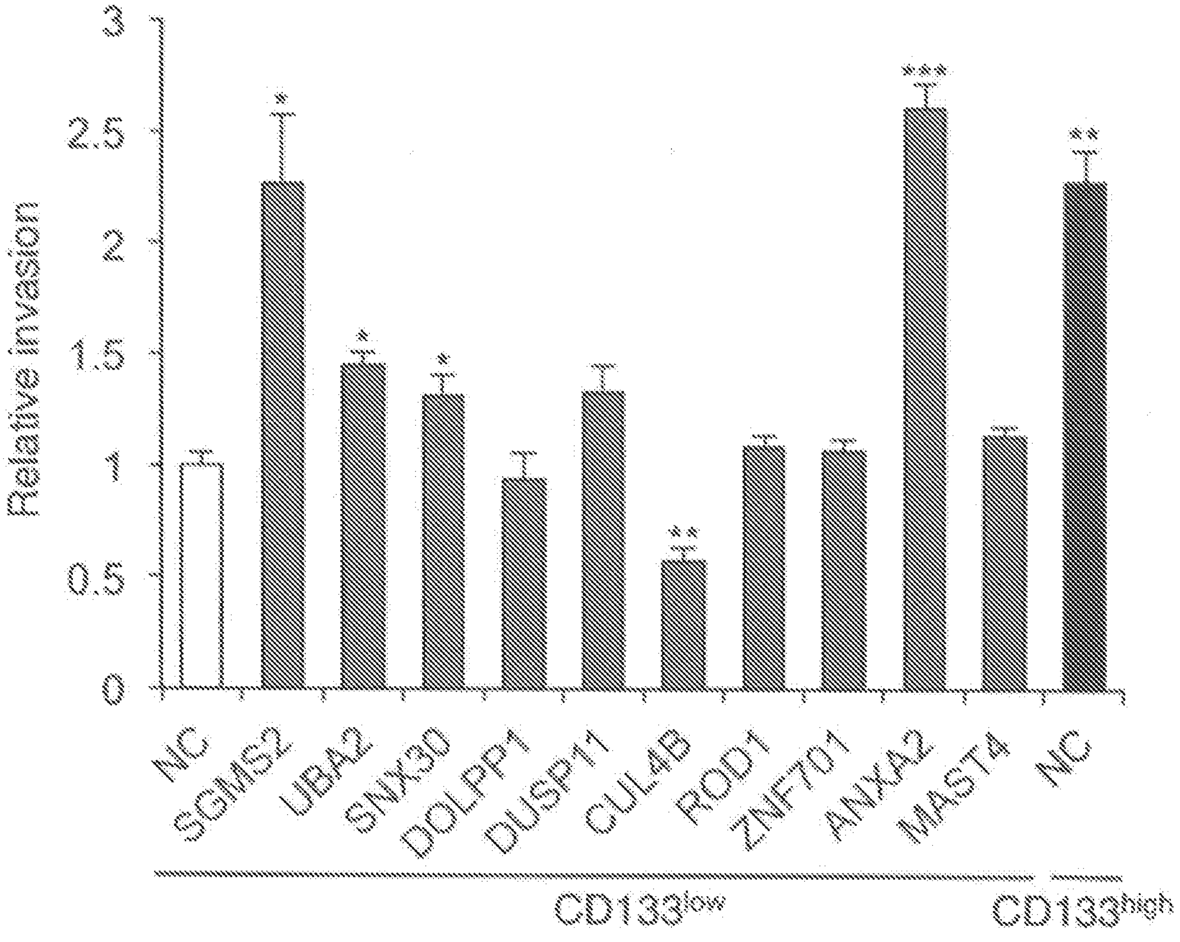
Relative invasion
3
2.5
2
1.5
1
0.5
0
*
*
*
**
***
**
NC
SGMS2
UBA2
SNX30
DOLPP1
DUSP11
CUL4B
ROD1
ZNF701
ANXA2
MAST4
NC
CD133^low
CD133^high

Fig. 39

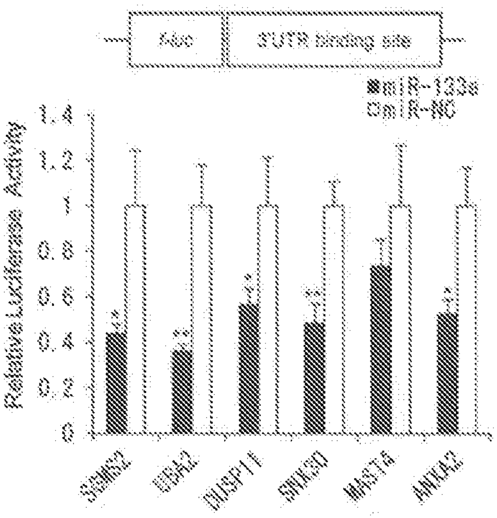
hluc
3'UTR binding site
■miR-133a
□miR-NC
Relative Luciferase Activity
1.4
1.2
1
0.8
0.6
0.4
0.2
0
**
**
**
**
**
SGMS2
UBA2
DUSP11
SNX30
MAST4
ANXA2

Fig. 40

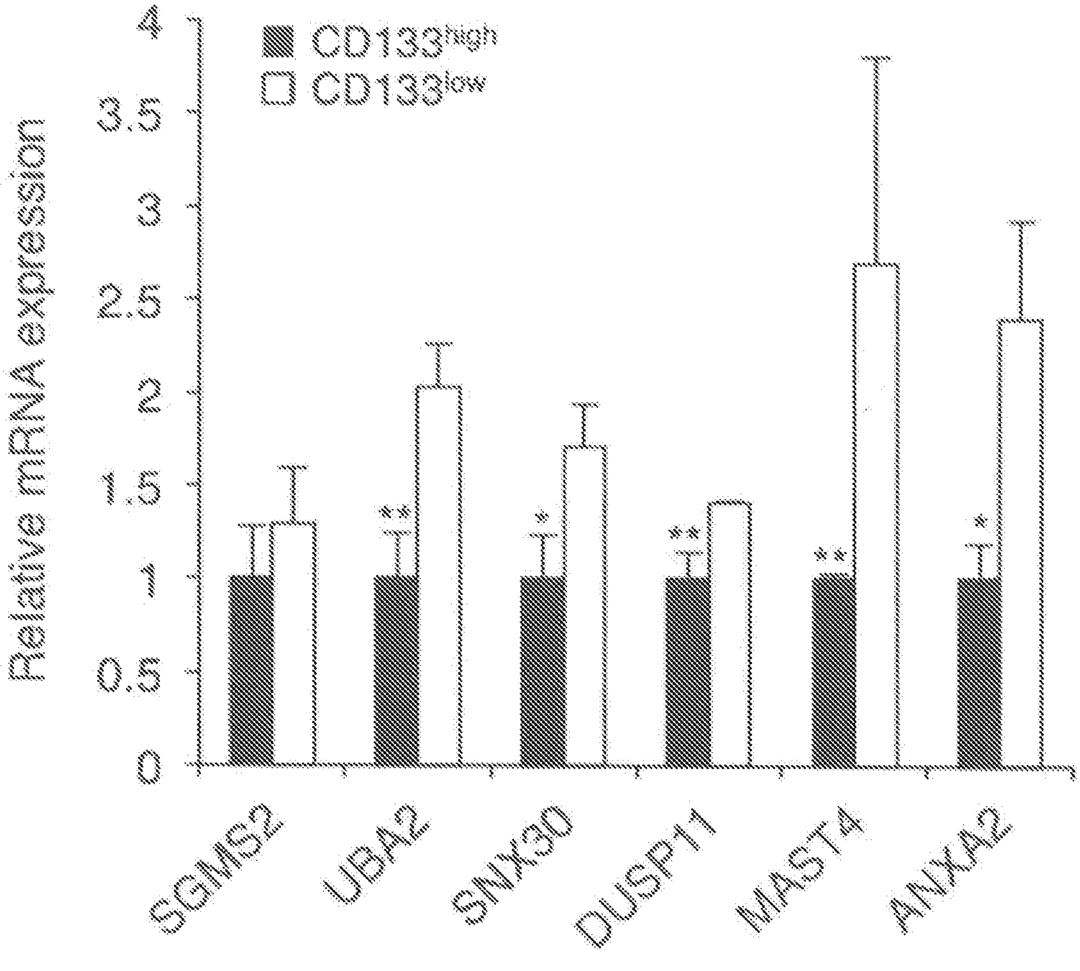
CD133^{high}
CD133^{low}
Relative mRNA expression
4
3.5
3
2.5
2
1.5
1
0.5
0
**
*
**
**
*
SGMS2
UBA2
SNX30
DUSP11
MAST4
ANXA2

Fig. 41

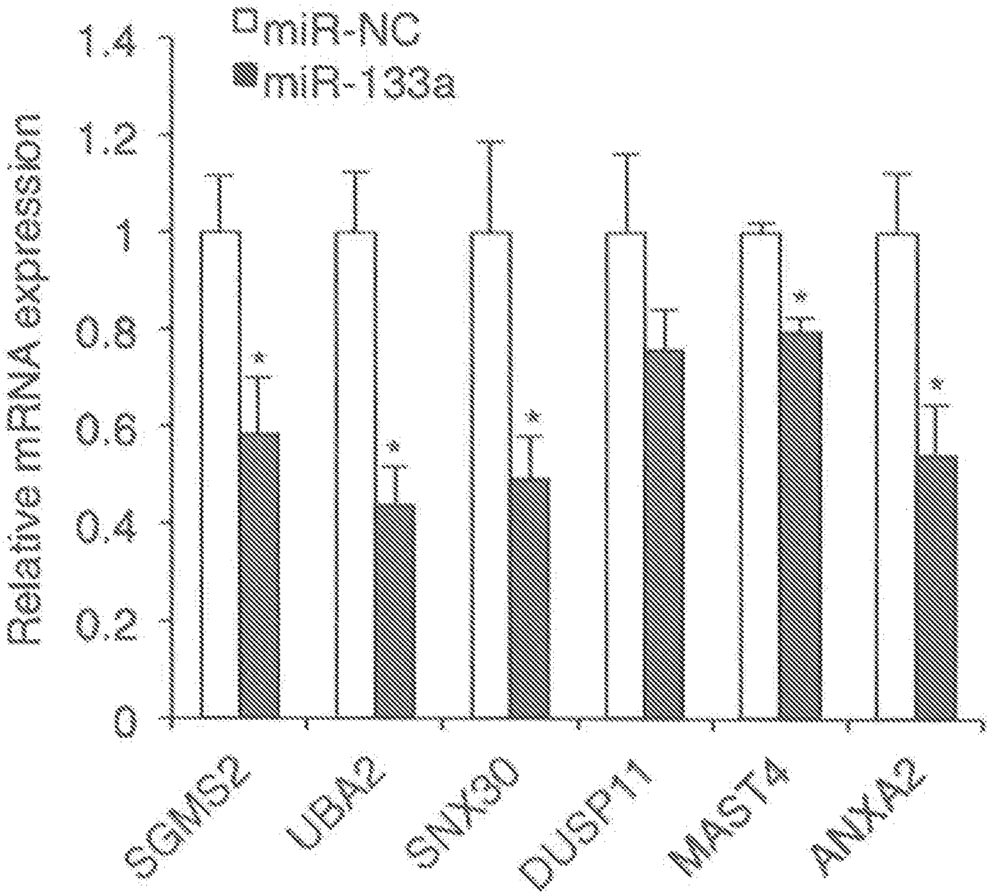
□miR-NC
▨miR-133a
Relative mRNA expression
1.4
1.2
1
0.8
0.6
0.4
0.2
0
*
*
*
*
*
SGMS2
UBA2
SNX30
DUSP11
MAST4
ANXA2

Fig. 42

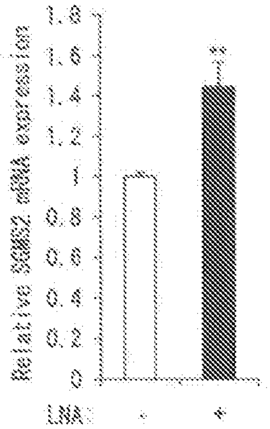

Fig. 43

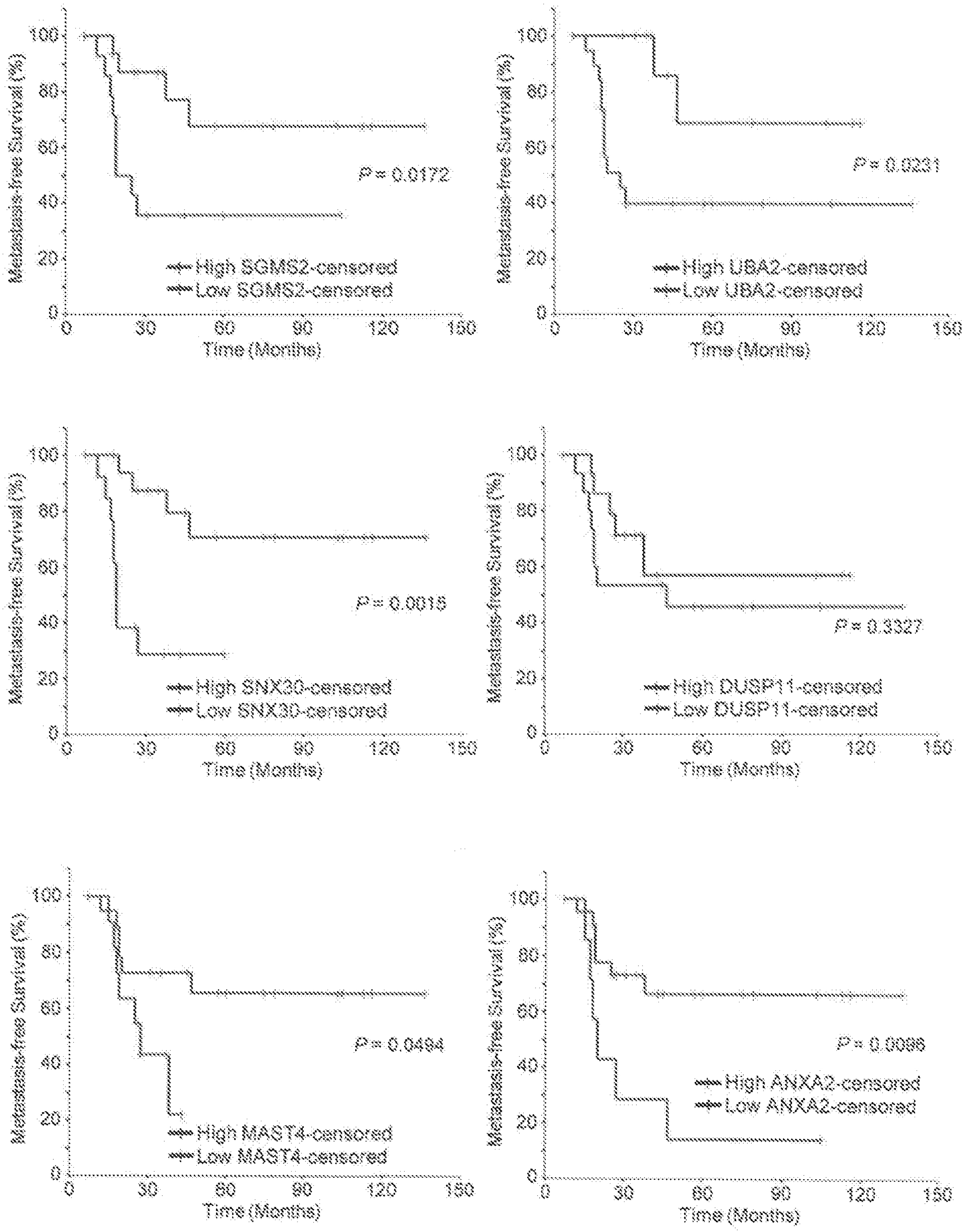
Metastasis-free Survival (%)
100
80
60
40
20
0
Time (Months)
0
30
60
90
120
150
P = 0.0172
High SGMS2-censored
Low SGMS2-censored
P = 0.0231
High UBA2-censored
Low UBA2-censored
P = 0.0015
High SNX30-censored
Low SNX30-censored
P = 0.3327
High DUSP11-censored
Low DUSP11-censored
P = 0.0494
High MAST4-censored
Low MAST4-censored
P = 0.0096
High ANXA2-censored
Low ANXA2-censored